BMI1 AND ITS ROLE IN PROMOTING BREAST CANCER TUMORIGENESIS

ROLE OF BMI1 IN PROMOTING BREAST CANCER TUMORIGENESIS THROUGH ATTENTUATING THE DNA DAMAGE RESPONSE PATHWAY

By
COLLEEN MacKENZIE, B.Sc. Honours

A Thesis

Submitted to the School of Graduate Studies

in Partial Fulfillment of Requirements

for the Degree

Master of Science

McMaster University
© Copyright by Colleen MacKenzie, June 2018.

MASTER OF SCIENCE (2018)

McMaster University, Hamilton, Ontario

Faculty of Health Sciences, Medical Sciences Graduate Program- Cancer and Genetics

TITLE:	Role of BMI1 in Promoting Breast Cancer Tumorigenesis Through Attenuating the DNA Damage Response Pathway
AUTHOR:	Colleen MacKenzie, B.Sc. (Queen's University)
SUPERVISOR:	Dr. Damu Tang
SUPERVISORY COMMITTEE:	Dr. Peter Whyte Dr. Khalid Al- Nedawi
EXTERNAL DEFENCE COMMITTEE MEMBER:	Dr. Jeremy Hirota
NUMBER OF PAGES:	xiv, 116

LAY ABSTRACT

Breast cancer (BC) is a complex disease with over 25,000 new diagnoses made in Canadian women every year. Normally there are anti-tumor mechanisms in place to protect against the abnormal cell division and growth that is associated with breast cancer. We propose a novel function of protein BMI1 to explain how breast cancer cells override these protective pathways. BMI1 is known to contribute to BC through inhibiting production of key tumor suppressing proteins and has recently been shown to decrease activity of the ataxia telangiectasia mutated (ATM)- mediated tumor inhibiting pathway. We propose a novel role of BMI1 in promoting breast tumor formation through inhibiting the ATM-mediated anti-tumor barrier, allowing cancer-promoting genes (oncogenes) to induce abnormal cellular growth. BMI1 was shown to be able to reduce oncogene induced ATM activity, in an action independent of established mechanisms. Additionally in MCF7 BC tumors, the presence of BMI resulted in a trend of reduction in ATM activity. Continued work to develop a transgenic mouse model with a breast specific BMI1 knockout will help further our understanding of BMI1's role in BC tumorigenesis.

ABSTRACT

Breast cancer (BC) is a complex disease with over 25,000 new diagnoses made in Canadian women every year. The disease can be caused by inactivation of the ataxia telangiectasia mutated (ATM) pathway, a major anti-tumor mechanism that protects against the abnormal cell division and growth that occurs in breast cancer, but how the pathway is inactivated has yet to be completely elucidated. BMI1 is an established oncogene that is overexpressed in BC and is associated with poor disease prognosis. BMI1 is a component of the polycomb repressive complex 1 (PRC1) that acts to repress transcription of the ARF/INK4A locus encoding two important tumor suppressor genes. We have recently shown a novel property of BMI1 in attenuation of ATM function independent of this locus. We thus hypothesize a role of BMI1 in promoting BC formation through inhibiting oncogene-induced ATM activation, allowing cancer-promoting genes to induce abnormal cellular growth. To examine this hypothesis, we transiently expressed oncogene c-Myc with or without BMI1 co-expression. As expected, ectopic c-Myc expression upregulated γH2AX, a demonstrated target of ATM; concurrent BMI1 expression reduced the γH2AX levels. Similar observations were also obtained using a BMI1 mutant deficient in promoting PRC1-mediated repression of the ARF/INK4A locus. These observations support the concept that BMI1 contributes to ATM inactivation during BC tumorigenesis through mechanisms independent of PRC1. To further examine this concept, we investigated the association of γH2AX and BMI1 in vivo. In MCF7 cell-produced xenograft tumors, the presence of γH2AX nuclear foci was clearly observed, indicative of ATM activation during BC tumorigenesis. In xenografts

generated by MCF7 cells stably expressing BMI1, a trend of reduction in γH2AX nuclear foci was observed. To further model BMI1's pathological relevance in c-Myc induced BC under a more physiological setting, we are developing transgenic mouse models (GEM) with breast-specific c-Myc expression with or without a breast-specific BMI1 knockout. The goal of these experiments is to recapitulate the above in vitro and in vivo observations. The expectation, should it be achieved, will significantly strengthen the connection between BMI1 and ATM during breast cancer tumorigenesis.

ACKNOWLEDGEMENTS

I would first and foremost like to thank Dr. Damu Tang for giving me the opportunity to be his graduate student over the past two years. I could not have asked for a better supervisor to help instill a love and respect for research in me. Dr. Tang's passion and enthusiasm towards research is admirable, and even when I was faced with the many difficulties that research has to offer his continuous support and insight was invaluable. I have learned more from Dr. Tang than I have room to write and I will forever be grateful for the time I have spent as one of his students.

To both of my committee members Dr. Peter Whyte and Dr. Khalid Al- Nedawi, thank you both for your encouragement and insight into my research, I appreciate all the time you have both spent on my project.

To Dr. Diane Ojo, and Dr. Xiaozeng Lin, thank you both for being so patient and encouraging while teaching me all of the new techniques that I needed over the past two years. You have both been incredible mentors and I will take what you have both taught me and use it far into the future. I would also like to thank the rest of the Tang lab- Yan Gu, Dr. Wenjuan Mei, Yanzhi Jiang, Kuncheng Zhao, David Rodriguez, Marc Ramkairsingh, and Mathilda Chow- for their continuous support. Knowing that at least one member of our lab, whether it be at 11 pm or on the weekend, will be at St. Joe's to keep me company has made all the hard work we do enjoyable even when things get tough.

To my parents, I will forever by thankful for the love and support that you have always had for me. You have both shown me what it means to work hard and love what you do and I hope one day that I will grow to become just as incredible as you two are. To my brothers Iain and Michael, I feel blessed to have two siblings like you. You both inspire me on the daily and I am honestly in constant awe of how smart, humble, and kind you both are. I am thankful every day for the family I have been blessed with and I could not have completed this academic journey without the four of you.

The last two years working on my graduate degree have involved some difficult yet rewarding experiences. This time has shown me how important medical research is to future advancements in health care and how important constant learning and discovery is to scientific endeavor. I am honored to have been a part of a group of individuals who are so dedicated and passionate about scientific research and I look forward to using the collective knowledge I have learned here in the future.

TABLE OF CONTENTS

LIST OF FIGURES

LIST OF TABLES

LIST OF ABBREVIATIONS

ATM	Ataxia- telangiectasia mutated
ATMpS1981	Phosphorylation of ATM at serine 1981
ATR	Rad3- related
BC	Breast Cancer
BER	Base excision repair
BMI1	B- cell specific Moloney murine leukemia virus integration site 1
BRCT	Breast cancer C- terminal domain of NBS1
BSA	Bovine serum albumin
CRE	Cre recombinase
DAPI	4',6- diamidino-2-phenylinodole
DDR	DNA damage response
DEGs	Differentially expressed genes
DEPC	Nuclease free water
DMEM	Dulbecco's modified eagle's medium
DNA	Deoxyribonucleic acid
DNA-PK	DNA dependent protein kinase
DSB	Double stranded breaks
E3-Ub	E3- ubiquitin ligase
ETOP	Etoposide
EV	Empty vector
FBS	Fetal bovine serum

FHA	Forkhead associated domain of NBS1
G_0	Growth zero phase
G_1	Gap 1 phase
G_2	Gap 2 phase
GEM	Genetically engineered mouse
GFP	Green fluorescent protein
GP	Gag-pol expressing vector
HR	Homologous recombination
HT	Helix-turn-helix-turn-helix-turn domain of BMI1
IR	Ionizing radiation
M	Mitosis
MDC1	Mediator of DNA damage checkpoint 1
MMR	Mismatch repair
MMTV	Mouse mammary tumor virus
Mo-MLV	Moloney murine leukemia virus
MRN	MRE11-RAD50-NBS1 complex
NER	Nucleotide excision repair
NHEJ	Non homologous end joining
NLS	Nuclear localization signal domains of BMI1
PBS	Phosphate buffered saline
PcG	Polycomb group
PCR	Polymerase chain reaction

PEST	Proline serine rich domain of BMI1
PIKK	PI3 kinase related kinase
PRC1	Polycomb repressive complex 1
RF	Ring finger domain of BMI1
ROS	Reactive oxygen species
RT	Room temperature
rtTA	Reverse tetracycline- controlled transactivator
S	Synthesis
s.c.	Subcutaneous
SNP	Single nucleotide polymorphism
TBS-T	Tris buffered saline
tetO	Tetracycline operator
TRITC	Tetramethylrhodamine
UV	Ultraviolet
VSV-G	Envelope expressing vector
WT	Wild type
γH2AX	Phosphorylation of histone H2AX at serine 139

DECLARATION OF ACADEMIC ACHIEVEMENT

Although I was the major contributor for the work presented in this thesis, this work required collaboration from several individuals.

Dr. Damu Tang and I designed the experiments and provided technical input on this project. Dr. Dianne Ojo provided the MCF7 xenograft tumors used for this analysis. Dr. Xiaozeng Lin created the BMI1 domain deletion mutants used for the transient expression experiments, and Dr. Wenjuan Mei provided assistance in creating the MCF7 stable lines. Kelly MacNeill provided training and initial assistance in breeding the transgenic mice. I performed the experiments, mouse breeding, analyzed the data and prepared figures and tables for this dissertation.

CHAPTER 1: INTRODUCTION

1.1 Overview of Breast Cancer

1.1.1 Breast Cancer Epidemiology

Cancer is the leading cause of death in Canada, accounting for 30% of all Canadian deaths (1). According to Canadian Cancer Statistics (2017) 1 in 2 Canadians will develop cancer within their lifetime, with 1 in 4 Canadians expecting to die due to this disease. Worldwide, BC is the most commonly diagnosed cancer in women, and is the second most common cause of cancer death in females, accounting for 13% of all female cancer deaths. It is shown that Canadian females are more likely to develop BC than any other cancer, excluding non-melanoma skin cancer, with 1 in 8 females expected to develop BC in their lifetime. In Canada there are over 25,000 new BC diagnoses made every year, accounting for approximately 26% of cancer diagnoses in Canadian women. The majority of BC cases occur in women younger than 70 years old, but BC causes a higher proportion of female cancer deaths in the younger age group of 30-59 where it is responsible for 21% of all female cancer deaths in this group. This is possibly linked to this age group displaying a more aggressive tumor biology on average (2) and delayed diagnosis (3,4). Although mortality rates have declined 44% since they peaked in 1987 due to significant advances in BC mammography screening and improvement in effective treatment, BC incidence rates have remained relatively stable (5,6). BC will remain a major contributor to the burden of cancer in the Canadian population with there being a

predicted 55% increase in cases from the mid-2000s to 2030 (7). This is largely attributed to our limited understanding of the etiology of BC.

1.1.2 Characterization of Breast Cancer

Breast cancer (BC) is a multifaceted disease with many components playing a direct role in its development. Most BC cases are diagnosed through identification of an abnormal or new lump or mass within the breast through screening techniques, such as mammography. BC is defined as a group of malignant cells that arise from cells lining the ductal system of the breast (ductal carcinoma) or from cells of the lobules of the breast (lobular carcinoma). BC is a heterogeneous disease that clinically can be classified based on the receptor expression of the estrogen receptor (ER), progesterone receptor (PR), and the hormone epidermal growth factor receptor 2 (HER2/neu). The majority of BC cases are ER+, accounting for approximately 75% of all cases, with most additionally being PR+ (8,9). Most current hormone therapies are designed to target the ER through endocrine therapy and block ER signaling through selective estrogen receptor modulators (SERMs), estrogen biosynthesis inhibitors (aromatase inhibitors/AIs), and selective estrogen receptor regulators (SERDs) (10). The HER2 gene encodes for an important receptor on breast cells that controls cell growth, division, and repair, and in approximately 20% of BC cases there is an overexpression of the HER2 receptor, resulting in the aggressive and fast growing BC type, designated HER2+. HER2+ BC cases are less likely to be sensitive to hormone therapy, but HER2- directed treatments, such as Trastuzumab, are shown to be more effective (11). In Triple negative (TN) BC

the ER, PR, and HER are not found to be present in the cancer tumor, and it is responsible for 10-20% of diagnosed breast cancers. Due to this cancer type lacking the necessary receptors for hormone therapy, this common treatment is ineffective (12). Although TN BC is considered more aggressive and difficult to treat due to its increased tendency to spread and recur, chemotherapy is usually the most effective treatment plan for TN BC. BC can be further classified based on gene expression profiles. Six intrinsic subtypes have been identified as luminal A and B (ER+), normal- like, Her2- enriched, basal like (TN), claudin low (TN) (13). BC displays traits such as uncontrolled proliferation, insensitivity to negative growth regulation, evasion of apoptosis, invasion and metastasis, and angiogenesis. These oncogenic properties are due to alterations within multiple pathways and networks. A major mechanism contributing to these changes is genomic elasticity, a hallmark characteristic of breast cancer (7).

1.1.3 Genomic Instability, a Hallmark of Breast Cancer

Cancer-associated genomic elasticity results from a loss in genome stability. Maintenance of genome integrity is an essential task for normal human cells under division. This is due to consistent damage by a variety of genotoxic insults that are either generated internally during cellular processes or come from externally generated sources. Regardless of origin, DNA lesions are efficiently repaired by the DNA damage response (DDR) pathway. DDR is an essential aspect of cell proliferation as its proper activation ensures that DNA damages are fixed prior to completion of cell division. The DDR pathways being compromised can lead to the fixation of DNA lesions in cells, ultimately

contributing to genome instability (14). Tumor cells are more genetically unstable compared to normal cells, and it is thought that the initiation and progression of normal cells to one of a cancerous phenotype is triggered by acquired genomic alterations that can collect over numerous cell divisions (15). Normally anti-tumor mechanisms are in place to counter this oncogenic force through promptly identifying and repairing mutations within the genome to maintain proper cell function and survival, thus decreasing dysregulation of cellular division.

1.1 The DNA Damage Response Pathway

1.2.1 Types of DNA Damage and their Repair Mechanisms

DNA is constantly being modified and damaged in numerous ways, which threatens genome stability and integrity. These lesions can arise endogenously through normal physiological processes (like the production of ROS) as well as exogenously through environmental DNA damaging events. Due to its chemical structure DNA is particularly susceptible to spontaneous hydrolysis reactions that result in deamination, and ongoing cellular metabolism naturally results in the generation of reactive oxygen species (ROS) that can create a variety of lesions such as double stranded breaks (DSB), with both leading to a loss in genomic stability (16). DNA is constantly assaulted by a number of additional exogenous mutagens such as ultraviolet (UV) light, ionizing radiation (IR), X-rays, radioactive substances, and chemotherapeutic drugs that can collectively result in chemical induced base modifications, interstrand crosslinks, and single and double- strand breaks. Due to there being a wide range of potential DNA lesions several well-established repair pathways such as nucleotide excision repair (NER), base excision repair (BER), mismatch repair (MMR), non homologous end joining (NHEJ), and homologous recombination (HR) are utilized to repair DNA damage and maintain genomic integrity.

DNA lesions formed through UV light chemicals and certain exogenous and chemotherapeutic chemicals are repaired through nucleotide excision repair (NER). NER acts through the coordination of more than 25 proteins to replace modified nucleotides

(17). Through several steps this repair system is able to recognize the lesion, excise the damaged DNA, synthesize new DNA, and ligate the corresponding flanking regions. Defects within this pathway have been associated with diseases such as Cockaynes disease, and various types of cancer (18).

Base excision repair (BER) mechanisms are responsible for the replacement of modified bases that are altered through deamination, methylation, and oxidation. These base modifications often occur due to spontaneous chemical reactions and ROS- induced DNA lesions. DNA glycosylase enzymes function to recognize and remove structurally changed bases from the genome and replace them by utilizing rapidly synthesizing polymerase and ligase enzymes (19).

Exogenous and endogenous agents can additionally cause base deamination, oxidation, and methylation with the mismatch repair (MMR) system functioning to remove resultant base mismatches. MMR additionally acts to repair insertion/ deletion and replication error derived base mismatches. Replication errors naturally occur at a rate of one incorrect nucleotide per 107 additions and MMR works to recognize these lesions, and excise and repair the base pair mismatch (15). Unfortunately not all mistakes generated through DNA replication errors can be repaired through MMR, with approximately 0.1% of these mismatched resulting in more permanent genetic mutations (20).

DSBs can be one of the most detrimental types of DNA damage, as presence of DSBs can result in cell death if they inactivate any essential genes for cell survival, and are intrinsically more difficult to repair due to erroneous rejoining of DNA (21, 22). Depending on the cell-cycle status of the damaged cells DSB repair occurs through two different processes, non homologous end-joining (NHEJ) or homologous recombination (HR). NHEJ occurs during the G_0/G_1 phase and works to ligate broken DNA strand ends, but this pathway is seen as error- prone due to a lack of a homologous sequence control system with deletion, inversions, and other abnormalities possibly resulting from the process (23). Conversely HR acts to repair DSBs during the S-G_2/M phase transition and is considered an error-free DNA repair mechanism as it repairs the broken ends dependent on a homologous template DNA sequence (24). Defects within DSB repair machinery are shown to lead to premature aging, neurodegeneration, and increased cancer susceptibility (16). Thus, a thorough understanding of how this process may go awry is of utmost importance.

Regardless of the type of lesion and the respective repair mechanisms it is critical that DNA damage is rapidly identified and repaired to counteract the inherent DNA damage that develops through a cell's lifetime. Maintenance of diverse DNA repair pathways is critical when conserving genomic integrity as seen with the dysregulation of these repair mechanisms resulting in significant clinical consequences. These DNA repair processes are tightly linked to pathways that detect and promote repair of these lesions, collectively deemed the DNA damage response (DDR). A critical component of DDR is the

utilization of cell cycle checkpoints that act to monitor the extent of DNA damage within a cell, the rapidity of repair, the stage of the cell cycle, and the strength of participating DDR components and ultimately determine whether cell cycle arrest, programmed cell death, or senescence should occur. In addition to DNA damage checkpoints, DDR activates DNA repair pathways, promotes the movement of DNA repair proteins to sites of DNA damage, activates transcriptional programs, and can induce cell death through apoptosis (25, 26).

1.2.2 Cell cycle checkpoints

To further maintain genomic stability during cell division a number of surveillance systems, deemed cell cycle checkpoints, are used to monitor both internal and external cues to decide whether cell division should proceed. Upon detection of DNA lesions, cell cycle checkpoints are activated to stop cell cycle progression and allow for DNA repair before cell division events continue. These DDR processes primarily act through the coordinated work of three apical PI3 kinase related kinase (PIKK) family members, ataxia-telangiectasia mutated (ATM), RAD3-related (ATR), and DNA dependent protein kinase (DNA-PK) (27). ATR is primarily activated through the formation of single-stranded breaks while ATM and DNA-PK are activated through the presence of double stranded breaks (DSBs) (25, 28).

1.2.3 Ataxia-telangiectasia mutated's role in DDR

Due to the detrimental nature of DSBs, ATM's role as a central transducer in DDR is of utmost importance. Activation of ATM by DSBs results in the coordinated action of various effectors systems that work together to counteract genotoxic stressors and events. ATM is a serine/ threonine protein kinase that plays a key role in regulating these responses and has been shown to play a part in more than 700 protein responses in result of DNA damage, showcasing how ATM is involved in a vast network of protein interactions (29). The activation of ATM to induce cell cycle checkpoints can result in the growth arrest of damaged cells in the G2/M phase to allow for the DNA damage to be repaired and for cells to once again resume normal function and cell cycle progression (30).

ATM activation is required for its function. Both autophosphorylation of ATM at serine site 1981 (pS1981) and binding to the MRE11/RAD50/NBS1 (MRN) complex through association with NBS1 is required for ATM activity (31). Activated ATM directly phosphorylates several important downstream substrates such as p53 and CHK2 (32, 33). The p53 tumor suppressor is crucial in a signal transduction network that triggers appropriate responses in face of DNA damage, thus minimizing tumorigenic potential. ATM- mediated phosphorylation of its serine site-15 is critical in stabilization of p53. In situations of DNA damage, p53 activation can hinder cell proliferation to prevent further DNA damage and promoate repair, or can result in programmed cell death or senescence when DNA damage is beyond repair to avoid the possibility of malignant transformation

(34). ATM activates CHK2, a threonine kinase, through phosphorylation at its threonine site-68, which directly results in downstream phosphorylation of CDC25A, marking it for proteasomal degradation, inhibiting its ability to dephosphorylate CDC2 at its tyrosine site-15. This initiates cell cycle arrest by disrupting the function of CDC2, a critical protein kinase needed for initiation of DNA synthesis and cell cycle progression (35).

ATM binding to the MRN complex is also a key factor behind HR in response to DSBs. MRE11/RAD50 binding to DSBs recruits ATM through its direct association with NBS1 where ATM can produce γH2AX, the phosphorylated version of histone H2AX at its serine site-139. The creation of γH2AX is necessary for DNA repair as it provides the site for docking of DSB repair proteins in the DSB surrounding region (36). This results in successive recruitment of MDC1 (mediator of DNA damage checkpoint 1) which in turn is phosphorylated by casein kinase 2, and further enables association of the ATM/MRN complex through NBS1 binding (37, 38). This complex leads to the spreading production of γH2AX along the DSB surrounding region and recruitment of multiple E3- ubiquitin ligases that play a critical role in cell commitment to HR mediated DSB repair (39, 40).

ATM- mediated DDR is of great importance for the repair of DSBs as is supported by evidence showing that mutations in this critical DDR protein can lead to loss in motor function, immune deficiencies and high frequencies of cancer development (41, 42). The ATM- mediated DDR pathway is considered an anti-tumor barrier as it is frequently

activated to maintain the genomic integrity of a cell and prevent progression to malignancy. This pathway can be triggered by the abnormal expression of tumor promoting genes, or oncogenes, to inhibit the hyper proliferation that is a key characteristic of BC cells (14).

1.2.4 Oncogene induced DNA damage response

Genomic instability characterizes all human cancers, and contributes to activation of oncogenes and inactivation of tumor suppressors. Activation of oncogenes induces a loss of heterozygosity and genomic stability in mammalian cells, human xenografts, and mouse models (43). Although it has been argued that oncogenes do not directly induce genomic instability, through promoting cell proliferation oncogenes can cause replication stress that impacts genome integrity (10). This model theorizes that genomic instability is generated by DNA replication stress due to oncogene-induced elevation of proliferation rate. Replication stress is characterized by a destabilization of appropriate replication ability as seen through a deceleration or stalled replication fork progression, with both inducing genomic instability (44).

This is supported by evidence that uncontrolled activity of E2F group transcription factors activate ATM dependent growth arrest, showcasing that elevated DNA replication is considered a DNA stressor that triggers DDR events (45,46). p53 additionally has a high frequency of mutation in human cancers, with oncogene- induced DNA damage possibly being responsible for this trend (10). Typically in precancerous lesions that retain p53

function oncogene-induced DNA damage elicits apoptosis or senescence to minimize growth of the lesion. When there is a loss of function in p53 cells are shown to escape this protective mechanisms and the precancerous lesion retains the ability to become cancerous (45, 47).

This is evidence that DDR activation can lead to proliferation arrest as a type of tumorigenic barrier. Somehow this is bypassed through alterations in cellular processes to promote tumorigenecity (48). Since ATM phosphorylation directly results in p53 activation it has been suggested that this loss of function may result from a disruption in ATM- mediated DNA DDR-response that is activated in response to oncogene-induced hyperproliferation (14). How and by what means this anti- tumour mechanism may be overcome is of great interest in understanding the mechanisms behind tumorigenesis.

1.3 BMI1 as an oncogene

1.3.1 Identification of BMI1 as an oncogene

B- cell specific Moloney murine leukemia virus integration site 1, commonly deemed BMI1, was first identified in 1991 by two separate research groups (49, 50). Both teams identified it to cooperate with c-Myc, an influential transcription factor that regulates approximately 15% of all human genes with its activation tightly linked to cell growth, proliferation, metabolism and apoptosis, in accelerated B-lymphoid tumor formation (51, 52). These qualities make c- Myc an important factor when considering the abnormal proliferation of cancerous cells. At the time of BMI1 identification c-Myc function was not fully established, but its dysregulation was implicated in oncogenesis.

To identify unknown genes that might act in conjunction with c-Myc both groups used retroviral insertional mutagenesis, a powerful screening tool used for the identification of oncogenic mutations. Moloney murine leukemia virus (Mo-MLV) was utilized to promote tumorigenesis as it was theorized that this virus would insert near or within possible cellular oncogenes, thus tagging genes that may promote B- lymphoid tumor formation. From Mo-MLV derived tumors provirus spanning sequences were cloned and a common locus was found, thereafter deemed BMI1, to be contained in nearly 50% of the tumors (49). Although the function of BMI1 was not exactly known at the time, both groups additionally showed a diverse expression of BMI1 transcripts in a number of normal tissues such as hematopoietic tissue, and tissues of the salivary glands, testis, heart, brain and kidney. Using a structural analysis of the gene sequence, several motif

characteristics of common transcriptional regulators were found to be present. Specifically the N-terminus was found to contain a putative zinc-finger with similar homology to several nuclear binding proteins as well as a nuclear localization signal, and a sequence high in proline, glutamic acid, serine and threonine (PEST).

This initial identification of BMI1 as a novel zinc-finger transcriptional regulator set the tone for subsequent analysis of its role in tumorigenesis. Since then it has been shown to play an important role in a variety of cancers and is not only upregulated in BC (53, 54) but also lymphomas (55, 56), prostate (57), colon (58), cervical, ovarian (59), and brain cancers (60, 61), with expression being associated with poor disease prognosis. BMI1 is involved in a number of oncogenic activities such as epithelial- mesenchymal transition, an important process needed for tumor progression (62), the generation of BC stem cells where it promotes stemness through being involved in stemness related genes and represses genes that induce cellar senescence and cell death (63), and promotion of cell immortalization and proliferation (64, 65).

1.3.2 BMI1's role in PRC1

BMI1 has since been established as a component of the polycomb repressive complex 1 (PRC1) (66). PRC1 is one of two classes of polycomb repressive complex, with both polycomb group (PcG) proteins founds to play a major role in transcriptional regulation (67). It has been well established that PcG proteins contain intrinsic enzymatic activity that facilitates the covalent modification of histones, demonstrating activity at the

chromatin level (66). The PRC1 complex has additionally been shown to possess H2A-K119 ubiquitin E3 ligase activity, suggesting this may be involved in its ability to maintain long term gene silencing (68). PRC1's E3- ubiquitin ligase contains several PcG proteins including RING1/ RING1a, RING2/RING1b, and BMI1. RING2/ RING1b has been established as the catalytic subunit of PRC1, and although it does not have enzymatic activity on its own, BMI1 binding to RING2 through its ring finger (RF) domain is required to activate PRC1's E3-ubiquitin ligase (69).

Histone ubiquination is a critical process needed for DSB repair through HR and NHEJ. BMI1 contributes to H2A and H2AX ubiquination through its role in activating PRC1's E3-ubiquitin ligase. This activity partially underlies BMI1's oncogenic activity. Ubiquination of H2A at K119 is a well-established mechanism that represses gene transcription and facilitates DSB repair. Additionally it is observed that BMI1 facilitates BRCA1 recruitment, an essential component needed for successful HR in response to DSBs. A role of BMI1 in recruiting essential proteins needed for DSB-elicited NHEJ is also shown (70). Evidence shows BMI1 recruitment is required for DNA damage induced ubiquination, resulting in promoter repression in active transcriptional regions near DSBs (66), with loss of BMI1 leading to impaired repair of DSB through HR (71). Active transcription is a constant threat to genome integrity, and the ability for DSBs to repress transcription in flanking regions is essential for proper DSB repair that does not further compromise this. Although the structural details involved in the process are yet to

be demonstrated, structural analysis supports the concept that BMI1 mediated ligase activity is important to its role in DSB repair.

Additionally BMI1-mediated E3-ubiquination of histone H2A is involved in the repression of key tumor suppressors encoded by the INK4A-ARF locus (72). INK4-ARF, also known as CDKN2A is expressed in many tissue and cell types and encodes for the production of two tumor suppressors $p16^{INK4A}$ and $p19/14^{ARF}$, both being tightly involved in growth arrest, senescence, and apoptosis (73, 74). $p16^{INK4A}$ activity inhibits cyclin dependent kinases 4 and 6 (CDK4 and CDK6) by activating pRb to result in eventual inhibition of G1/S phase progression. pRb is known as a key regulator of cell-cycle transition and repression or inactivation of pRb function in tumorigenesis can be a consequence of both direct and indirect disruption within the pathway. $p19/ p14^{ARF}$ blocks MDM2 inhibition of tumor suppressor p53, inducing G1 and G2 checkpoint arrest. Mutation of p53 is thought to be one of the most frequent genetic alterations seen in human cancer (75). Collaboration between the INK4A-ARF encoded pRb and p53 pathways is critical in tumor suppression as is demonstrated by multiple tumor types exhibiting disruption in both pathways. BMI1- mediated repression of this locus by PRC1 E3-ubiqutin ligase activity contributes to BMI1's tumorigenic potential. However, the INK4A-ARF locus is mutated in approximately 75% of cancers, with BMI1 retaining its oncogenic activity in cancer cells where this locus is disrupted (76). Interestingly, additional evidence has shown that BMI1's transcriptional repression can be separated from this oncogenic activity (77). BMI1's role in PRC1 thus clearly contributes to

tumorigenesis through enhancing DSB repair thus possibly playing a role in the resistance of cancer therapy, and through suppression of key tumor suppressors, but whether this is its only, or even major role is unlikely.

1.3.3 BMI1 attenuation of checkpoint activation

Checkpoint activation is an important aspect of DDR and the coordination of ATM and its downstream targets is critical in its maintenance. Ectopic expression of BMI1 is established to reduce γH2AX, an established biomarker of DSBs and their repair, in IR treated keratinocytes, with a knockdown significantly increasing levels in cisplatin-treated A-2780 and CP70 cells, two ovarian cancer cell lines, suggesting a role of BMI1 in attenuating DSB- mediated checkpoint activation (78,79). A novel contribution of BMI1 in reducing ATM activation has been reported that is independent of known PRC1 E3- ubiquitin ligase activity. Etoposide (ETOP), a common drug used to induce DSBs as a cancer therapy, was used to explore a possible role of BMI1 in MCF7 breast cancer and DU145 prostate cancer cells (80). It was shown that ectopic expression of BMI1 significantly decreased ETOP induced γH2AX levels, an established biomarker of DSBs, and conversely the knockdown of BMI1 in these cell lines rescued γH2AX production and nuclear foci formation (80). These effects were reproduced in non-cancerous MCF10A mammary epithelial cells in response to ETOP treatments. In line with DSBs recruiting ATM through MRN complex association and subsequent γH2AX formation in proximate DSB regions, overexpression of BMI1 reduced ETOP- induced ATM activation and phosphorylation of downstream target CHK2, with knockdown of BMI1

reversing this affect (80). In addition to this, G2/M phase arrest was reduced in ETOP-treated MCF7 cells that overexpress BMI1. Collectively these observations demonstrate that BMI1 may help cells better survive ETOP induced G2/M checkpoint activation through attenuation of ATM activity in breast and prostate cancer cells.

In response to how BMI1 may alter ATM activity it was demonstrated that BMI1 expression alters NBS1-ATM association (80). The MRN complex made of Mre11, Rad50 and NBS1 is of critical importance for ATM mediated DSB repair, as it is through ATM's known binding to NBS1 that allows it to be recruited to DNA lesions and promote DNA repair (81). Thus it is likely that this novel association contributes to BMI1's inhibition of ATM activation. To further characterize this interaction, deletion mutants of BMI1's ring finger (RF), helix-turn-helix-turn-helix-turn (HT), proline/ serine rich (PEST), and nuclear localization signal (NLS) domains were created. Co-expression of individual deletion mutants RF and HT with NBS1 showed retained association, meaning these two domains do not have a major role in the BMI1-NBS1 interaction, while still retaining their ability to attenuate ATM activation (80). This is of utmost importance because it is the RF domain that is required to bind PRC1's catalytic subunit RING2 to activate its E3-Ub, thus indicating a role of BMI1 independent of PRC1's E3-ubiquitin ligase activity in attenuating ATM (82). NBS1 holds two functional domains connected through a flexible linker, N terminal phosphoprotein binding core with a forkhead- associated domain (FHA) and the breast cancer C-terminal (BRCT) domain (83-85). The C-terminal core domain includes binding motifs for MRE11 and ATM (86,

87), but presently it is unclear in what manner BMI1 interacts with NBS1, and how this interaction in turn influences DSB- induced ATM activation.

1.3.4 BMI1's collaboration with other oncogenes in tumorigenesis

It is well established that the over-expression of oncogenes can trigger DDR and result in cell cycle arrest as an anti-tumor barrier. BMI1 was originally identified as an oncogene through its cooperation with c-Myc during leukemogenesis (49, 50), and c-Myc directly transactivates BMI1 in leukemia, neuroblastoma, and nasopharyngeal carcinoma (88-90) to ensure the presence of BMI1 in further facilitation of c-Myc oncogenic functions. Additionally BMI1 collaborates with other oncogenes such as Ras (91), Abl (89), and hTERT (92). The mechanisms underlying this collaboration have yet to be elucidated. It is possible that BMI1's transcriptional repression of the INK4A-ARF locus through PRC1 participation contributes to its collaboration with c-Myc during tumorigenesis (93). Conversely this collaboration may also be through ATM inhibition, where E3- ubiquitin ligase activity is not required. The upregulation of BMI1 (14), activation of common oncogenes such as c-Myc and Ras (54), and inactivation of ATM-mediated DDR (94) all have the commonality of displaying oncogenic activity in BC. This suggests an interesting model where BMI1 may inhibit oncogene-induced ATM- DDR events to allow for cancer progression. This is supported by evidence of BMI1 collaboration with RasV12 in the transformation of MCF10A cells to form xenograft tumors (95).

1.4 Genetically engineered mouse (GEM) models

1.4.1 Genetically engineered mouse models in cancer research

Mouse models are an integral component to further understand the pathogenesis behind tumor formation, and can allow for insight into the disease that in vitro experiments cannot answer. With advancement in these systems comes a better understanding behind mechanisms such as cancer initiation, immune system response, tumor angiogenesis, invasion, and metastasis, and the importance of molecular diversity in human cancer, all allowing for better therapeutic and diagnostic strategies to be developed. Although there are many differences between mice and humans, as mammals both share many anatomical, cellular, and molecular traits that are critical to tumorigenesis, such as an immune system, maternal effects in utero, imprinting of genes, and alternative splicing (96). Over 100 years of genetic mouse research has resulted in powerful strategies for assessing the complex genetics of disease and associated therapeutic responses among human populations. Hypotheses that originate in an in vitro environment can be tested for further validity by utilization of the mouse model.

Research using animal models has been an essential part in improving therapies for BC as well as in better elucidating mechanisms behind BC development. Profiling the pathological relevance of a disease is essential for classification, prognosis and disease management, so maintenance of genetic complexity and tumor pathology is essential in genetic models (97). In vivo analysis capitalizes on the mouse as a physiologically relevant system to model BC initiation, invasion and metastasis, and represents an

intermediate in-between in vitro and clinical study work (98). An expansive number of models are now available that reflect different BC subtypes and disease stages (99). Cell-line derived xenografts have been shown to be extremely useful in assessing breast cancer genetics, biological processes, and to some extent metastatic potential, but its use is limited by their reduced intra-tumoral heterogeneity, inability to predict clinically useful therapies, and the use of this technique to model native tumor environments is limited (100). Although xenograft models are not applicable for predictive strategies for targeted BC therapies, they still remain very useful prior to analysis in more complex models.

Genetically engineered mouse (GEM) models have proven to be an affective tool in addressing many of these issues surrounding xenograft models as it involves the de novo studying of tumorigenesis, and thus is the system of choice for cell- intrinsic and cell-extrinsic processes that contribute to cancer initiation, progression, and metastasis. The early 1980s showed the first creation of oncomice where their genome contained cloned cancer genes; specifically the transgenic expression of activated oncogene v-HRAS under the control of a mammary specific promoter, MMTV that drives mammary tumorigenesis (101). Due to transgene expression being ubiquitous in the tissue types there were limitations to how this model could mimic sporadic cancer formation. To correct this issue more complex models were developed to allow for somatic inactivation of tumor suppressor, or activation of oncogenes (102).

1.4.2 Cre- loxP System

Due to past limitations in using conventional GEM models that drive transgene expression, models better emulating the genetics of human disease have been developed that contain spatial and temporal transgene activation or deletion. This modeling technique allows for a more developed understanding behind the biological basis of cancer development and growth. One conditional GEM models utilizes the Cre/ loxP system, a site specific recombinase technology that drives expression and resultant targeted gene splicing in specified tissue types. This system utilizes bacterial enzyme Cre recombinase to result in recombination between target sequences denoted as loxP sites. Proper placement of loxP sequences allows for the activation, repression, translocation and inversion of specific genes of interest. Cre activity can be under control of specific promoters as to be expressed in designated cell types or to be triggered by external stimulus. One of the original examples of a successful utilization of such a system was the generation of a mouse colorectal cancer model using Cre-loxP inactivation of the gene APC, with a loss resulting in the rapid onset of colorectal adenomas (103). Introducing mutations associated with specific cancer types can generate mouse models that better replicate histopathological, molecular, and clinical features of tumorigenesis (104).

1.4.3 c-Myc inducible BC model to study BMI1 collaboration

A GEM model can be utilized to further study the pathological relevance of BMI1. The original oncomice experiments provided evidence that oncogene expression leads to tumorigenesis (101). Oncogene expression can alternatively be regulated through an

inducible system. Tetracycline inducible techniques are established to activate oncogenes and induce tumorigenesis (105). This is evidenced by the continuous expression of a tetracycline derivative, doxycycline, inducing the MYC transgene in hematopoietic cells to result in the formation of malignant T-cell lymphomas and acute myeloid leukemia that regressed with re-induction of MYC (106). It has additionally been established that c-Myc under a tetracycline inducible promoter (tetO- MYC) causes BC in mice when crossed to MMTV-rtTA mice (107). The mouse mammary tumor virus (MMTV) long terminal repeat promoter is well established to drive a high level of Cre recombinase expression in the luminal epithelial cells of the breast (107, 108). Mice that have a floxed BMI1 gene ($BMI1^{loxp/loxp}$) have been previously utilized in the modeling BMI1 requirement in intestinal cancer tumorigenesis (109). Using these two defined techniques to create a mouse model that expresses breast specific c-Myc expression, and a breast specific knockout of BMI1 will be of interest to further elucidate BMI1's role in BMI1 tumorigenesis.

1.5 Central Hypothesis, Specific Hypotheses and Specific Aims

1.5.1 Main Thesis Question

Does BMI1 cooperate with oncogenes to overcome DDR anti-tumor barriers to promote BC tumorigenesis?

1.5.2 Main Thesis Hypothesis

BMI1 cooperates with oncogenes such as c-Myc during BC formation by inhibiting oncogene-induced ATM activity, thus promoting tumorigenesis.

1.5.3 Specific Objectives

To better elucidate BMI1's role in promoting BC tumorigenesis:

1) Evaluate BMI1's ability to regulate c-Myc induced γH2AX foci formation using wildtype BMI1 and deletion mutants BMI1ΔRF, BMI1ΔHT, BMI1ΔPEST, and BMI1ΔNLS. **2)** Create stable MCF7 lines expressing WT BMI1, or BMI1 deletion mutants BMI1ΔRF, BMI1ΔHT, BMI1ΔPEST, and BMI1ΔNLS in conjunction with c-Myc. **3)** Investigate if BMI1 significantly reduces γH2AX levels in vivo using MCF7 derived xenograft tumors and immunohistochemistry techniques. **4)** Develop a GEM model with c-Myc induced BC tumorigenesis and breast specific BMI1 knockout by first crossing transgenic lines to a congenic C57BL/6 background.

1.5.4 Specific Hypotheses

The following specific hypotheses are proposed for this study:

1) BMI1 and BMI1ΔRF expression will reduce c-Myc-induced γH2AX foci percentage.

2) Tumor formation and lung metastasis in BMI1/c-Myc and BMI1ΔRF/ c-Myc expressing mice will be accelerated compared to EV/ c-Myc. **3)** The C57BL/6 background percentage of all transgenic lines will increase over several generations of backcrossing.

CHAPTER 2: MATERIALS AND METHODS

2.1 In vitro cell manipulation

2.1.1 Cell culture

MCF7 breast cancer and 293T cell lines were obtained from ATCC and cultured in Dulbecco's Modified Eagle's medium (DMEM) (Sigma Aldrich) supplemented with 5% FBS (Sigma Aldrich) and 1% Penicillin- Streptomycin (Life Technologies) at 37°C.

2.1.2 Transient transfections

MCF7 cells were seeded for 70% confluency 24 hours before transfection. Cells were transfected with green fluorescent protein (GFP) and empty vector control (EV), BMI1, BMI1ΔRF, BMI1ΔHT, BMI1ΔPEST, or BMI1ΔNLS in conjunction with EV or c-Myc using Lipofectamine 3000 Reagent (ThermoFisher Scientific).

2.1.3 Retroviral infection

A retroviral infection protocol was used to produce stable lines expressing BMI1, BMI1ΔRF, BMI1ΔHT, BMI1ΔPEST, or BMI1ΔNLS with and without c-Myc. BMI1 domain deletion constructs were made by subcloning BMI1, BMI1ΔRF, BMI1ΔHT, BMI1ΔPEST, or BMI1ΔNLS into the pLNCX retroviral vector. Plasmid DNA was isolated and used to generate pLNCX, pLNCX-BMI1, pLNCX- BMI1ΔRF, pLNCX-BMI1ΔHT, pLNCX- BMI1ΔPEST, or pLNCX- BMI1ΔNLS by using a calcium phosphate transfection protocol. 293T cells were seeded to be 30% confluency 24 hours

before transfection. The transfection cocktail contained 0.22- μm filtered 2.5 M $CaCl_2$, MiliQ pure H_2O, and 2X HeBS as well as the appropriate retroviral plasmid, gag-pol expressing vector (GP; Stratagene), and an envelope-expressing vector (VSV-G; Stratagene). 48 hours after transfection the virus-containing medium was harvested, filtered through a 0.45-μm filter and centrifuged using a Sorvall RC 6+ centrifuge (Thermo Scientific) at 50,000 *g* for 90 minutes at 4°C to concentrate the retrovirus. The virus was suspended in DMEM and used to infect MCF7 cells for a 2-hour period. Virus was then aspirated and fresh DMEM was added. Three days after infection with pLNCX, pLNCX-BMI1, pLNCX- BMI1ΔRF, pLNCX- BMI1ΔHT, pLNCX- BMI1ΔPEST, or pLNCX- BMI1ΔNLS retrovirus, stable line selection pursued with 1 mg/ml of G418-neomycin (Sigma Aldrich) for 2 weeks. Secondary infection with c-Myc-pBABE virus, following the same protocol listed above, was performed on pLNCX, pLNCX-BMI1, pLNCX- BMI1ΔRF, pLNCX- BMI1ΔHT, pLNCX- BMI1ΔPEST, or pLNCX-BMI1ΔNLS stable lines and subsequently selected with 400 μg/ μl of Zeocin antibiotic (Invitrogen) for 2 weeks.

2.1.4 Immunohistochemistry and quantification of xenograft tumors

Xenograft tumors were deparaffinised in xylene, cleared in an ethanol series, and heat treated for 20 minutes in a sodium citrate buffer (1.47 g sodium citrate, 0.25 mL Tween dissolved in 500 mL of ddH_2O) at pH= 6.0 in a food steamer. Slides were incubated in blocking buffer (10% Normal Goat Serum, and 1% BSA in 1X phosphate buffered saline-PBS) for 1 hour at room temperature (RT). Primary antibodies specific for anti- γH2AX

(1:1500- Cell Signalling) were incubated with the sections overnight at 4°C overnight. Slides stained without any primary antibody were used as negative controls. Anti-rabbit biotinylated secondary IgG (1:200-) was then added to each section for 1 hour at room temperature. Vector ABC reagent (Vector Laboratories) was subsequently added according to manufacturer protocol. Washes were performed in-between steps with 1X PBS. Chromogen reaction was carried out with diaminobenzidine (Vector Laboratories) and counterstained with hematoxylin (Sigma Aldrich). Slides were then cleared and dehydrated in an ethanol series and covered with Cytoseal mounting medium (Vector). Images of three tumor sections for MCF7 EV and BMI expressing tumors were scanned using an Aperio ScanScope (Leica BioSystems). Total cell counts were performed using ImageJ 1.50i, and number of γH2AX positive cells were counted using Adobe Photoshop CC 2017. Percent of γH2AX cells in the population were calculated.

2.1.5 Western blot analysis

Cell lysates were prepared in lysis buffer solution (20 mmol/L Tris (pH 7.4), 150 mmol/L NaCl, 1 mmol/L EDTA, 1 mmol/L EGTA, 1% Triton X-100, 25 mmol/L sodium pyrophosphate, 1 mmol/L NaF, 1 mmol/L b-glycerophosphate, 0.1 mmol/L sodium orthovanadate, 1 mmol/L PMSF, 2 µg/mL leupeptin, and 10 µg/mL aprotinin). 50 µg of total cell lysate were loaded and separated by 10% SDS- PAGE gel and transferred onto Amersham hybond ECL nitrocellulose membranes (Amersham). Membranes were blocked with 5% skim milk for 1 hour at RT and incubated with the appropriate antibody at the indicated concentration overnight at 4°C. Membranes were then washed in 1X tris-

buffered saline (TBS-T) and were incubated with the appropriate HRP- conjugated secondary antibody for one hour at RT. Membranes were washed and signals were detected using an ECL Western Blotting Kit (Amersham).

The primary and secondary antibodies and the concentrations used were:

M2- flag (1:1000; Sigma Aldrich)

c-Myc sc-40 (1:200; Santa Cruz)

β- actin (1:1000; Santa Cruz)

α- tublin (1:1000; Santa Cruz)

anti- mouse IgG (1:3000; Bio Rad)

anti-goat IgG (1: 3000; Bio Rad)

2.1.6 Immunofluorescence staining and quantification

Immunofluorescence staining was performed to evaluate possible BMI1 effect on c-Myc induced γH2AX nuclear foci formation. Transient transfections were performed with the appropriate expressing vectors by the above-defined protocol in Nunc Lab-Tek chamber slides (ThermoFisher Scientific). 48 hours after transfection cells were fixed in 4°C paraformaldehyde (Affymetrix) for 10 minutes at room temperature followed by permeabilization with 0.3% Triton X-100 (Sigma Aldrich) for 15 minutes. Slides were then incubated in blocking buffer (3% BSA, 3% Donkey Serum, 0.1% Triton in PBS) for 1 hour at RT. Addition of primary antibody to anti- γH2AX (Cell Signalling, 1:100) was then performed at 4°C overnight. After washing with 1X PBS, TRITC- Donkey anti-

rabbit IgG (1:200, Jackson Immuno Research Lab) was applied for 1 hour at room temperature. Slides were then covered with 4',6- diamidino-2-phenylinodole (DAPI) mounting medium (VECTOR Lab Inc.) to stain cell nuclei. Images were taken with a fluorescent microscope (Carl Zeiss, Axiovert 200). GFP positive cells from 8-10 randomly selected fields of focus were imaged using a fluorescent microscope (Carl Zeiss, Axiovert 200) at X 40 magnification. Cells were analyzed for γH2AX foci formation. For analysis 150 GFP positive cells were used for analysis and the percent of γH2AX positive cells was calculated. Experiments were repeated 3 times.

2.1.7 Statistical analysis

Analysis was performed using Student's t-test (two-tailed), with a $p < 0.05$ regarded as statistically significant.

2.2 Animal work

2.2.1 Transgenic Mice

Tg(MMTV-Cre)4Mam/J (Stock number: 003553), B6;SJL-Tg(MMTV-rtTA)4-1Jek/J (Stock number: 010576), and Tg(tetO-Myc)36aBop/J (Stock number: 019376) transgenic mouse lines were obtained from Jackson Laboratory. $BMI1^{loxp/loxp}$ mice were obtained from Dr. Peter Whyte.

2.2.2 Mouse breeding

A trio- breeding scheme of one transgenic male mouse, and two female wildtype C57BL/6 mice was used to cross lines into the C57BL/6 background. Mice were determined to be pregnant from vaginal plug formation and pup palpitation, with mouse gestation lasting from 19-21 days. Pups were kept with the mothers until they were weaned at 21 days old, and separated by sex. From each cross the progeny were genotyped, according to the below protocol, for the appropriate transgene and the male mice deemed positive re-entered the breeding scheme once sexually mature at six weeks of age.

2.2.3 Mouse tissue collection and genotyping

Ear clip tissue samples were collected using a Fine Science Tools ear punch and digested in a solution of lysis buffer (1M TRIS-HCL, 20% SDS, 0.5 M EDTA, and 5M NaCL in ddH_2O) and 30 µl of proteinase K (20 mg/mL) over night at 55°C. An ethanol

precipitation was then performed by washing DNA samples with 100% ethanol, and subsequently with 70% ethanol at 4°C, then re-suspended in nuclease free water (DEPC). DNA concentrations were quantified using a spectrophotometer (NanVue Plus). Prepared DNA samples were run using a diagnostic PCR with TC-3000X PCR machine (Techne) according to PCR conditions supplied by Jackson Laboratories for each transgenic line. Between 15-20 ng/µl of DNA were loaded for each sample and were run on a 2% agarose gel. See Appendix I for PCR components and conditions:

Primers used for PCR:

Internal positive control (Forward): 5'-CTA GGCCACAGAATTGAAAGA CT-3'

Internal positive control (Reverse): GTAGGTGGAAATTC TAGCATCATCC-3'

MMTV-Cre (Forward): 5'-GCGGTCTGGCAGTAAAAACTATC-3'

MMTV-Cre (Reverse): 5'-GTGAAACAGCATTGCTGTCACTT-3'

TetO-Myc (Forward): 5'-TAGTGAACC GTCAGATCGCCTG-3'

TetO-Myc (Reverse): 5'-TTTGATGAAGGTCTCGTCGTCC-3'

MMTV-rtTA (Forward): 5'-GGCGAGTTTACGGGTTGTTA-3'

MMTV-rtTA (Reverse): 5'-CTGGTCATC ATCCTGCCTTT-3'.

2.2.4 Single Nucleotide Polymorphism (SNP) testing

Ear clip tissue samples from transgenic progeny were collected and sent to Jackson Laboratory for single nucleotide polymorphism (SNP) based genome screening to

confirm the congenicity of all three lines. Approximately 150 SNP regions are compared between samples and wildtype controls and the company provided a report.

CHAPTER 3: RESULTS

3.1 BMI1 and BMI1ΔRF reduce c-Myc induced ATM activation

Our group has previously shown that BMI1 attenuates ATM activation in MCF7 cells that were treated with DSB inducing agent etoposide; an action that was established to be independent of known BMI1 mediated E3-Ub ligase activity (80). Additionally we observed a role of BMI1 in enhancing resistance to Tamoxifen, an anti- BC drug, in ER+ breast cancer; intriguingly the BMI1ΔRF mutant that is defective in promoting PRC1's E3-Ub ligase activity (69) is as competent as WT BMI1 in conferring MCF7 cell resistance to Tamoxifen (9). These observations collectively support my hypothesis for BMI1-derived downregulation of ATM activity during BC tumorigenesis. This hypothesis is in additional accordance with some other well-established concepts. BMI1 was initially identified based on its collaboration with c-Myc in B- lymphoid tumorigenesis (49, 50). This collaboration seems a theme in BMI1-derived oncogenic activity involving other well-established oncogenes such as Ras (91), Abl (82), and hTERT (92), in addition to c- Myc. This collaboration can be attributable to BMI1-involved repression of the INK4A/ARF locus which encodes two critical tumor suppressors: p14ARF and p16INK4A; while the former activates p53, the latter stimulates pRb functions (73,74). The repression of the INK4A/ARF locus directly depends on BMI1-derived PRC1 E3-Ub ligase activity (72, 76). Nonetheless, evidence strongly suggests that BMI1 possesses oncogenic activities independent of this locus (see Introduction for details). Another important concept of tumorigenesis is the common activation of the ATM pathway by oncogenes, such as c-Myc, as an anti- tumor

mechanism (48), and the overall need to inactivate the ATM pathway (94). Our hypothesis suggests that BMI1 could collaborate with c-Myc in part through downregulation of the ATM pathway, and we will thus study this relationship in breast cancer, as both BMI1 and c-Myc are important oncogenic factors in BC tumorigenesis (14, 54).

To investigate the collaboration of BMI1 and c-Myc in BC tumorigenesis we examined the role of wildtype BMI1 and its deletion mutant BMI1ΔRF in MCF7 adenocarcinoma breast cancer cells through looking at the production of γH2AX nuclear foci using immunofluorescence techniques. The RF domain is required for binding of PRC1's catalytic subunit RING2 to activate E3-Ub (69), so utilization of this mutant can further elucidate independent activity. MCF7 cells were individually transfected with c-Myc, BMI1, BMI1ΔRF, c-Myc+BMI1 or c-Myc+ BMI1ΔRF along with green fluorescence protein (GFP) as an internal control (see later for details). The expression of these transgenes was demonstrated through western blotting (Figure 1). As expected, transfected cells evident by being GFP-positive, displayed strong γH2AX signal in the nuclei of c-Myc-transfected cells (Figure 2A); approximately 78% of cells transfected with only c-Myc were positive for nuclear γH2AX foci formation (Figure 2B). In comparison, the nuclear γH2AX was significantly reduced in cells co-transfected with c-Myc and BMI1 or BMI1ΔRF (Figure 2); ectopic expression of BMI1 alone was without effects on nuclear γH2AX (Figure 2). The c-Myc oncogene is well established to activate ATM (14) and γH2AX is a typical target of ATM (36). Collectively, the above results

support the possibility that BMI1 contributes to downregulation of the ATM pathway in response to c-Myc induced oncogenic activities independent of E3-Ub ligase activity.

A.

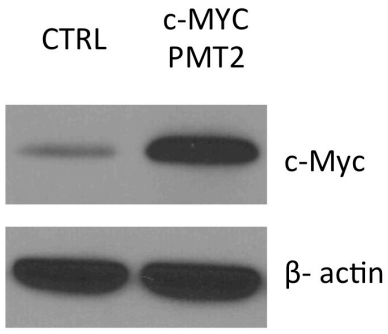

B.

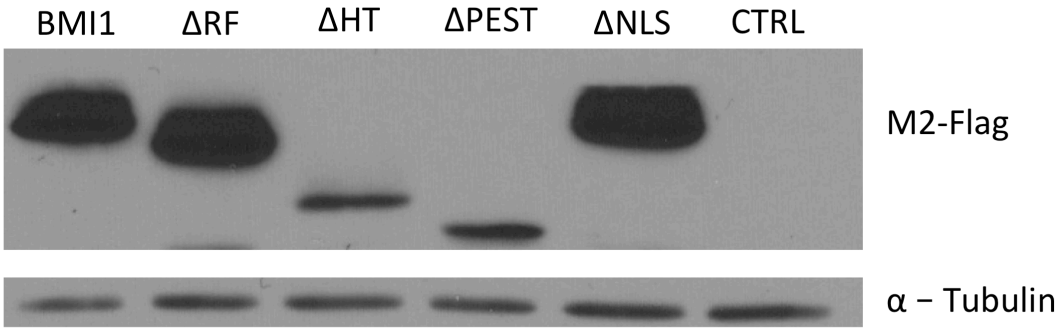

Figure 1. Overexpression of c-Myc, BMI1, and BMI1 deletion mutants in MCF7 cells. c-Myc, (A.) and BMI1, BMI1ΔRF, BMI1ΔHT, BMI1ΔPEST, or BMI1ΔNLS (B.) were overexpressed in MCF7 cells using Lipofectamine 3000 reagent protocol (see Materials and Methods for further details). BMI1 and domain deletion mutants are FLAG- tagged and examined by western blotting using M2- monoclonal anti- FLAG antibody (Sigma), and were different sizes due to domain deletion efforts. RF: ring finger, HT: helix- turn- helix- turn- helix- turn, PEST: proline/ serine rich domain, NLS: nuclear localization signals, CTRL: control.

A.

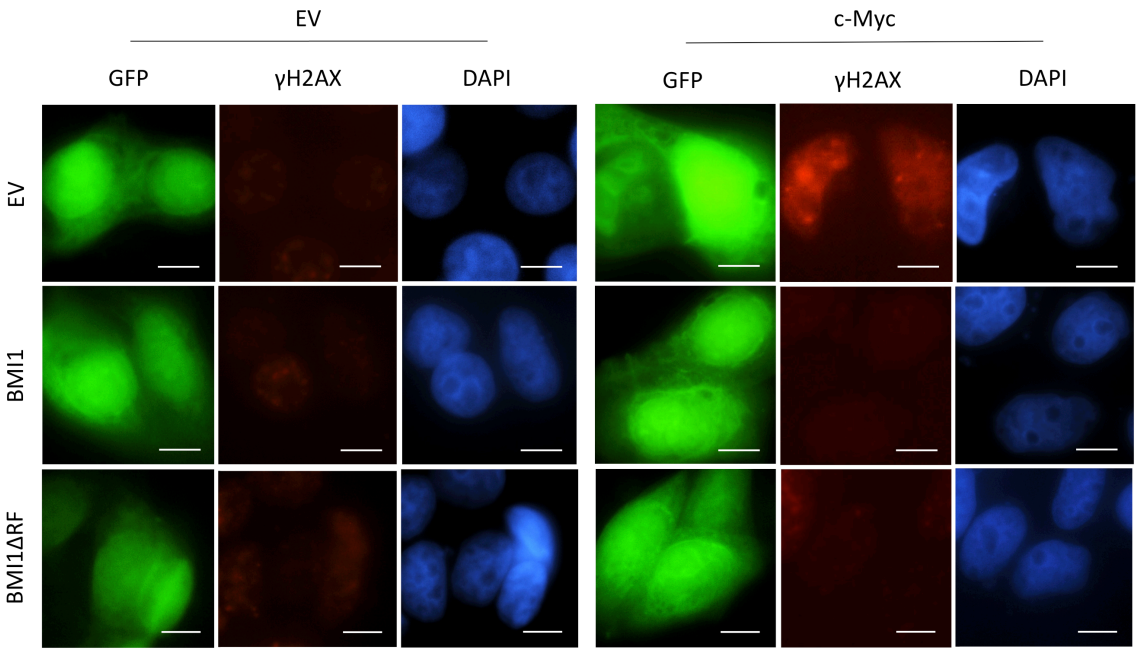
EV
c-Myc
GFP
γH2AX
DAPI
GFP
γH2AX
DAPI
EV
BMI1
BMI1ΔRF

B.

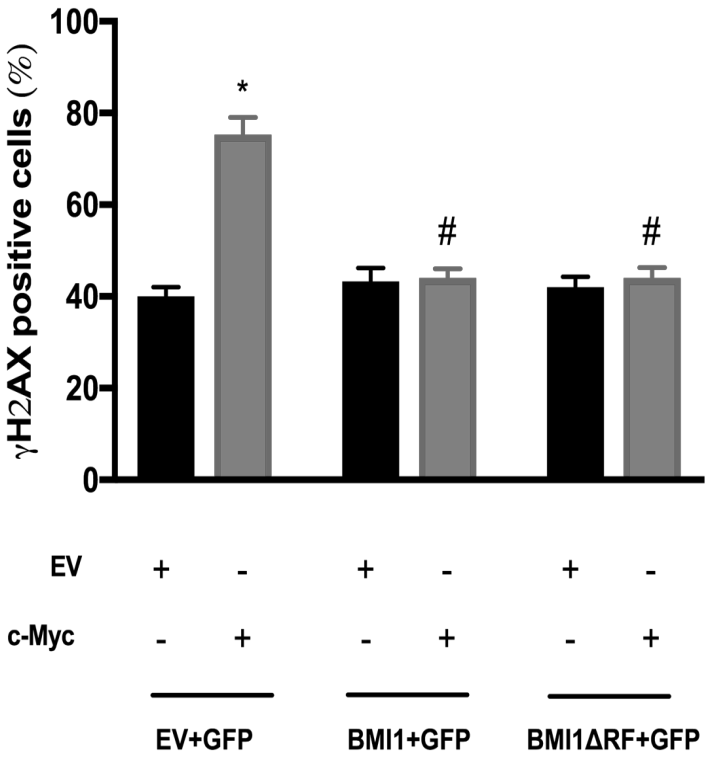
γH2AX positive cells (%)
100
80
60
40
20
0
*
#
#
EV + - + - + -
c-Myc - + - + - +
EV+GFP
BMI1+GFP
BMI1ΔRF+GFP

Figure 2. BMI1 and BMI1ΔRF reduce oncogene induced ATM activation. MCF7 cells were transfected with GFP (0.2 μg), empty vector (EV, 0.2 μg) and other indicated plasmids (0.2 μg each) for 48 hours, followed by immunofluorescence staining for γH2AX (red). (A.) A typical image of successfully transfected cells is shown and indicated through the presence of GFP (green), and nuclei were counterstained with 4',6-diamidino-2-phenylindole (blue); Scales bars, 5 μm. (B.) 50 GFP positive cells in randomly selected fields of focus were counted and percentages of γH2AX- positive cells in the GFP positive population were calculated. Experiments were repeated three times; mean ± SE (standard error) are graphed. *: $p<0.05$ in comparison to respective pBabe transfections (2- tailed student t- test); A#: $p<0.05$ in comparison to respective EV transfections (2- tailed student t- test). See Appendix II for descriptive statistics (Table 1), and independent t- test statistics (Table 2).

3.2 BMI1ΔHT, but not BMI1ΔPEST or BMI1ΔNLS reduce C-Myc induced ATM activation

BMI1 contains several other domains besides RF including helix-turn-helix-turn-helix-turn (HT), nuclear locational signals (NLS), and a proline/ serine (PEST) rich region. Our group has previously utilized these mutants in evaluating their contributions to BMI1-derived downregulation of ATM activation in etoposide- elicited DDR (Figure 3) (80). By taking advantage of these materials, I have analyzed the structural features of BMI1 involved in attenuation of c-Myc-induced nuclear γH2AX foci levels in MCF7 cells. These cells were transiently transfected with GFP alone with the indicated combination of c-Myc, EV, BMI1ΔHT, BMI1ΔPEST, and BMI1ΔNLS (Figure 4). Expression of c-Myc and the individual BMI1 mutants was demonstrated (Figure 1). Similar to BMI1, ectopic expression of individual BMI1ΔHT, BMI1ΔPEST, and BMI1ΔNLS did not induce nuclear γH2AX in MCF7 cells in comparison to cells transfected with EV (Figure 4). Co-expression of BMI1ΔHT fully reduced c-Myc-induced nuclear γH2AX to the basal level observed in EV-transfected MCF7 cells (Figure 4), suggesting BMI1ΔHT being as potent as BMI1 and BMI1ΔRF in downregulation of c-Myc-caused nuclear γH2AX (comparing Figures 2 and 4). The HT motif is likely dispensable to BMI1's activity in attenuation of c-Myc-induced ATM activation.

Deletion of either the PEST or NLS domain significantly compromised BMI1-derived reduction of nuclear γH2AX in MCF7 cells ectopically expressing c-Myc (Figure 4).

Nonetheless, neither mutant fully repressed c-Myc upregulated nuclear γH2AX (Figure 4). Evidence thus suggests that both motifs contribute to the BMI1's activity (Figure 3).

We have previously shown that BMI1ΔRF and BMI1ΔHT mutants retain the full level of activity in association with NBS1 and inhibition of ATM activation in etoposide-treated MCF7 cells (Figure 3) (80). BMI1ΔPEST and BMI1ΔNLS bind NBS1 with reduced capacity (Figure 3). These properties match well with the contributions of individual domains in downregulation of c-Myc-induced γH2AX in MCF7 cells (Figure 3). As binding to NBS1 is essential in ATM activation by double strand DNA breaks, the similar domain involvement in BMI1-derived attenuation of ATM activation caused by either etoposide or c-Myc (Figure 3) provides an additional support for BMI1 to reduce ATM activation caused by elevation in c-Myc expression.

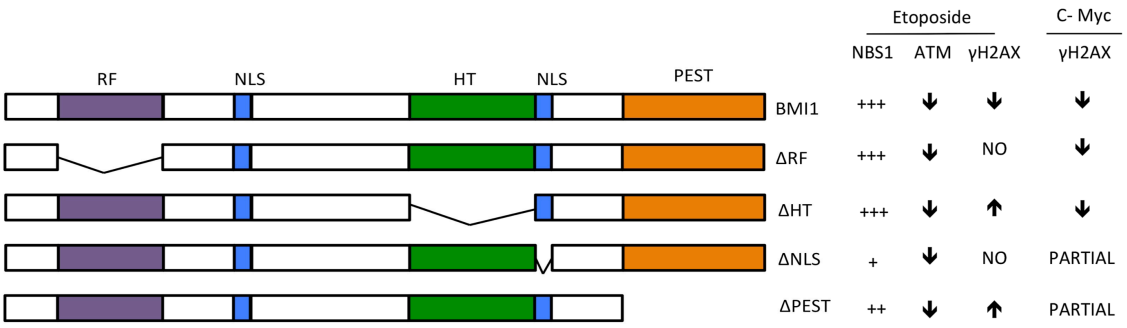

Figure 3. BMI1and domain deletion mutants show varied ability to down regulate etoposide and c-Myc induced γH2AX. BMI1 and the indicated deletion mutants are shown for their activities in binding to NBS1 and their ability to attenuate ATM activity. Additionally mutant ability to down regulate ATM activity has been evaluated for both etoposide and c-Myc treatments and resultant γH2AX levels were measured. RF: ring finger, NLS: nuclear localization signals, HT: helix- turn- helix- turn- helix- turn, PEST: proline/ serine rich domain; number of + symbols indicates binding affinity, up and down arrows indicate a decrease and increase of the indicated events, and NO: no effect.

A.

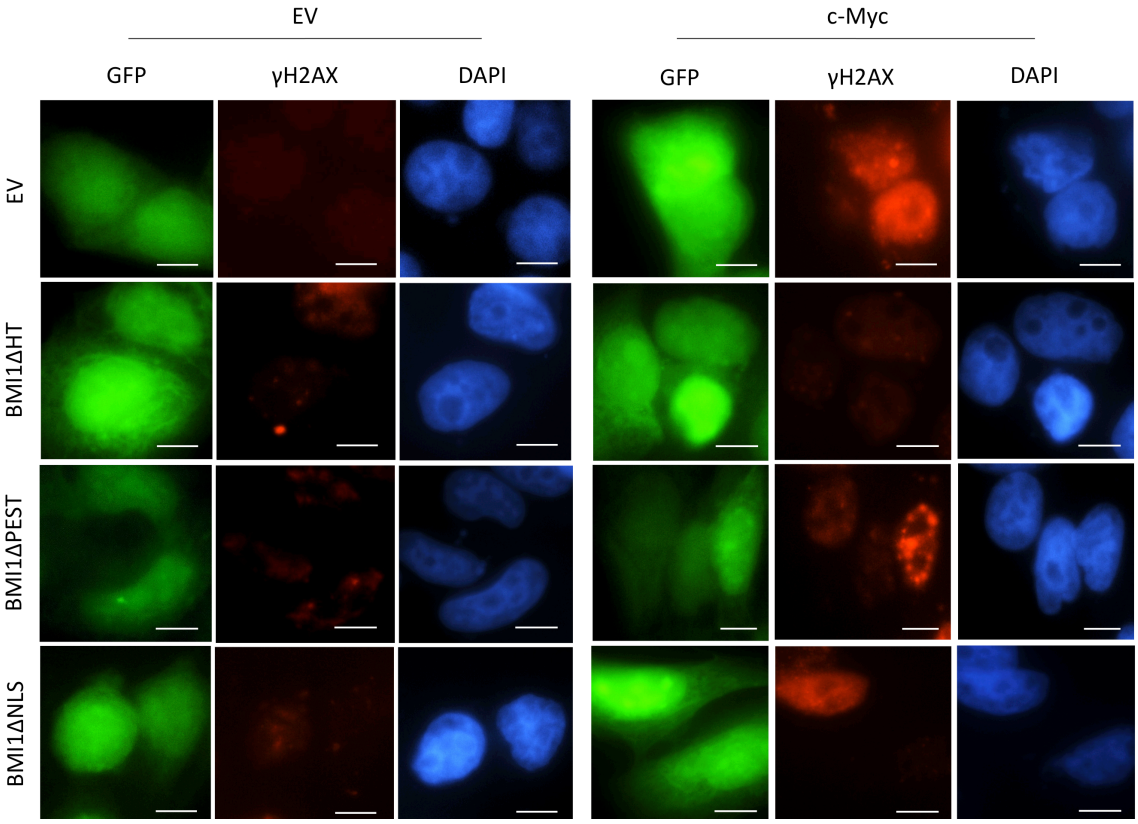
EV
c-Myc
GFP
γH2AX
DAPI
GFP
γH2AX
DAPI
EV
BMI1ΔHT
BMI1ΔPEST
BMI1ΔNLS

B.

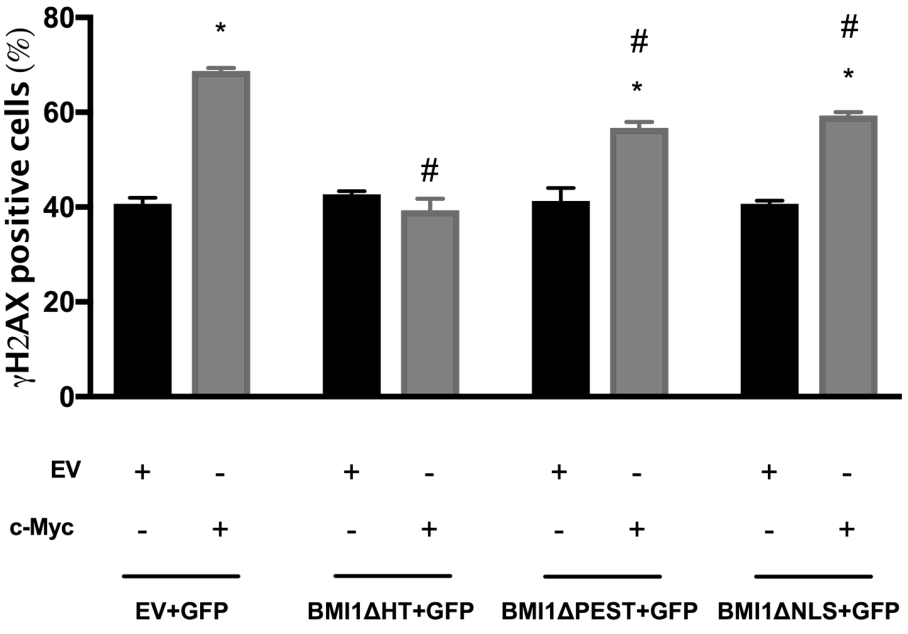
γH2AX positive cells (%)
80
60
40
20
0
*
#
#
*
#
*
EV + - + - + - + -
c-Myc - + - + - + - +
EV+GFP
BMI1ΔHT+GFP
BMI1ΔPEST+GFP
BMI1ΔNLS+GFP

Figure 4. BMI1ΔHT, but not BMI1ΔPEST, or BMI1ΔNLS reduce oncogene induced ATM activation. MCF7 cells were transfected with GFP and the indicated plasmids for 48 hours, followed by immunofluorescence staining for γH2AX (red). (A.) A typical image of successfully transfected cells is shown and indicated through the presence of GFP (green), and nuclei were counterstained with 4',6-diamidino-2-phenylindole (blue); Scales bars, 5 μm. (B.) 50 GFP positive cells in randomly selected fields of focus were counted and percentages of γH2AX- positive cells in the GFP positive population were calculated. Experiments were repeated three times; mean ± SE (standard error) are graphed. *: $p<0.05$ in comparison to respective pBabe transfections (2- tailed student t-test); A#: $p<0.05$ in comparison to respective EV transfections (2- tailed student t- test). See Appendix III for descriptive statistics (Table 1), and independent t- test statistics (Table 2).

3.3 BMI1 expression does not change γH2AX nuclear foci levels in MCF7 derived xenograft tumors

The above in vitro studies support a role of BMI1 in reduction of the ATM pathway during breast cancer tumorigenesis. We have previously reported continuous DNA damage is evidenced by the presence of γH2AX during tumorigenesis (110). We have recently demonstrated that BMI1 confers resistance to tamoxifen in ER+ breast cancer using xenografts generated by either MCF7 EV or MCF7 BMI1 (ectopically expressing BMI1) cells (9). We thus determined the γH2AX nuclear foci formation in xenograft tumors of either MCF7 EV or MCF7 BMI1 cells. Immunohistochemistry analysis was performed for MCF7 EV and MCF7 BMI1 derived tumors. Analysis of EV and BMI1 MCF7 xenograft tumors was performed using haematoxylin staining of cell nuclei and counterstaining for γH2AX nuclear foci. Both tumor types display γH2AX nuclear foci formation (Figure 5A). While there is a trend of less proportion of cells positive for γH2AX nuclear foci in xenografts produced by MCF7 BMI1 cells (Figure 5A), the difference was not statistically significant (Figure. 5B).

The non-significant status could be attributed to multiple factors. Based on the trend of reduction, it is highly possible that the sample size was two small. Secondly, the strength of oncogenic signals used to drive oncogenesis in this system may not lead to a high level of DNA damage; as a result the level of DNA damage is tolerable by tumors and there may not be a strong need to further reduce ATM activation. Both MCF7 cells proliferating slowly in vitro and the slow generation of xenografts in

immunocompromised mice support this possibility. Regardless, what might be the underlying causes, the actions of BMI1 in attenuation of ATM activation following BC tumorigenesis need to be further examined using a proper in vivo system.

A.

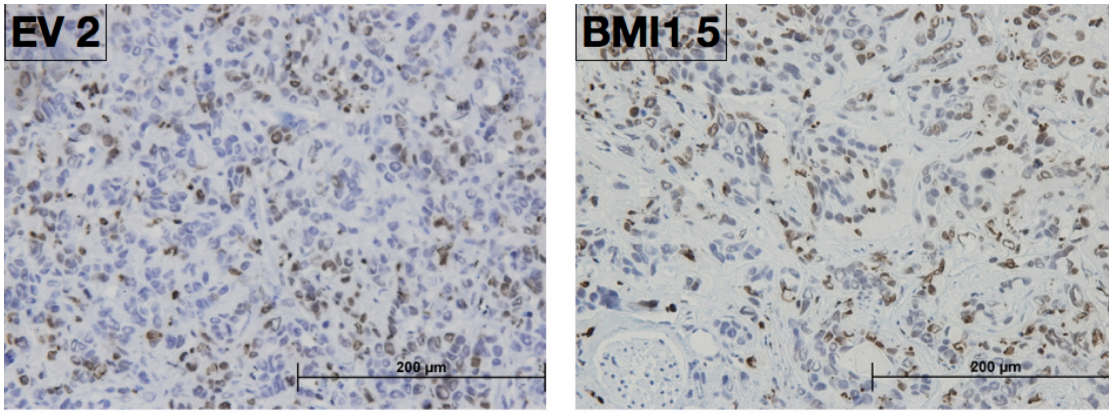

B.

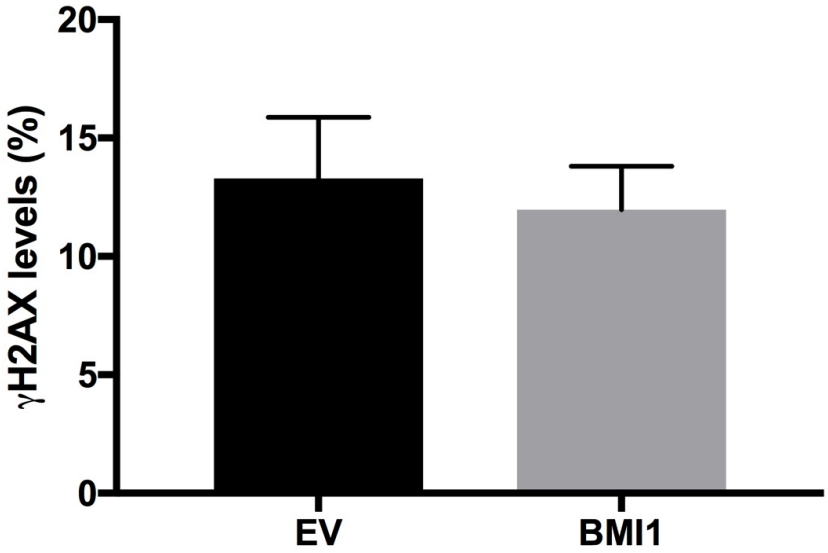

Figure 5. BMI1 and EV MCF7 xenograft have no significant difference in γH2AX nuclear foci levels. Immunohistochemistry analysis of EV and BMI1 stable expressing MCF7 derived xenograft tumors. (A.) A typical image of EV or BMI1 expressing tumors is shown. Cell nuclei staining was performed using haematoxylin and counterstaining for γH2AX nuclear foci. (B.) γH2AX nuclear foci levels were analyzed for EV (n=3) and BMI1 (n=3) xenograft tumors and percent of γH2AX nuclear foci to the total cell population was calculated (See Materials and Methods for details). Mean ± SE (standard error) are graphed. *p>0.05 (2- tailed student t- test), p=0.70. See Appendix IV for descriptive statistics (Table 1), and independent t- test statistics (Table 2).

3.4 Preparation of transgenic mouse lines to study BMI1 facilitating c-Myc-induced breast cancer through inhibition of ATM actions

To establish a proper in vivo system to examine the relationship between c-Myc and BMI1 with respect to ATM activation, we will use transgenic mice with breast specific expression of c-Myc with and without breast-specific knockout of BMI1, or c-Myc+BMI1. In brief, the system will involve the Cre-loxP system to direct breast specific BMI1 expression, the mouse mammary tumor virus (MMTV) to drive breast specific expression of rtTA, which will lead to breast specific expression of c-Myc driven by tetracycline-inducible promoter (tetO-Myc) (Figure 6). BMI1$l^{loxp/loxp}$ mouse line has been produced on a C57B/6 background, as supplied by Dr. Peter Whyte. The remaining three transgenic strains needed to create a mouse model that expresses breast specific c-Myc expression and a breast specific knockout of BMI1, MMTV-Cre, MMTV-rtTA, and tetO-Myc, were obtained on various strain backgrounds, FVB x B6129F1, C57BL/6 x SJL, and FVB x B6129F1 respectively (Table 1). These lines are being bred into a C57BL/6 background so experimental crosses can proceed. Due to the founding MMTV-Cre and tetO-Myc lines having low percentages of C57BL/6 in their background a predicted 5-8 total generations are needed to reach true congenicity. The original MMTV-rtTA founding line had a higher percentage of C57BL/6 and 3-5 generated of backcrossing is needed to reach true congenicity. Each line is at a different stage of backcrossing; presently we are on cross 6 for MMTV-Cre, 5 for tetO-Myc, and 4 for MMTV-rtTA (Figure 7).

A.

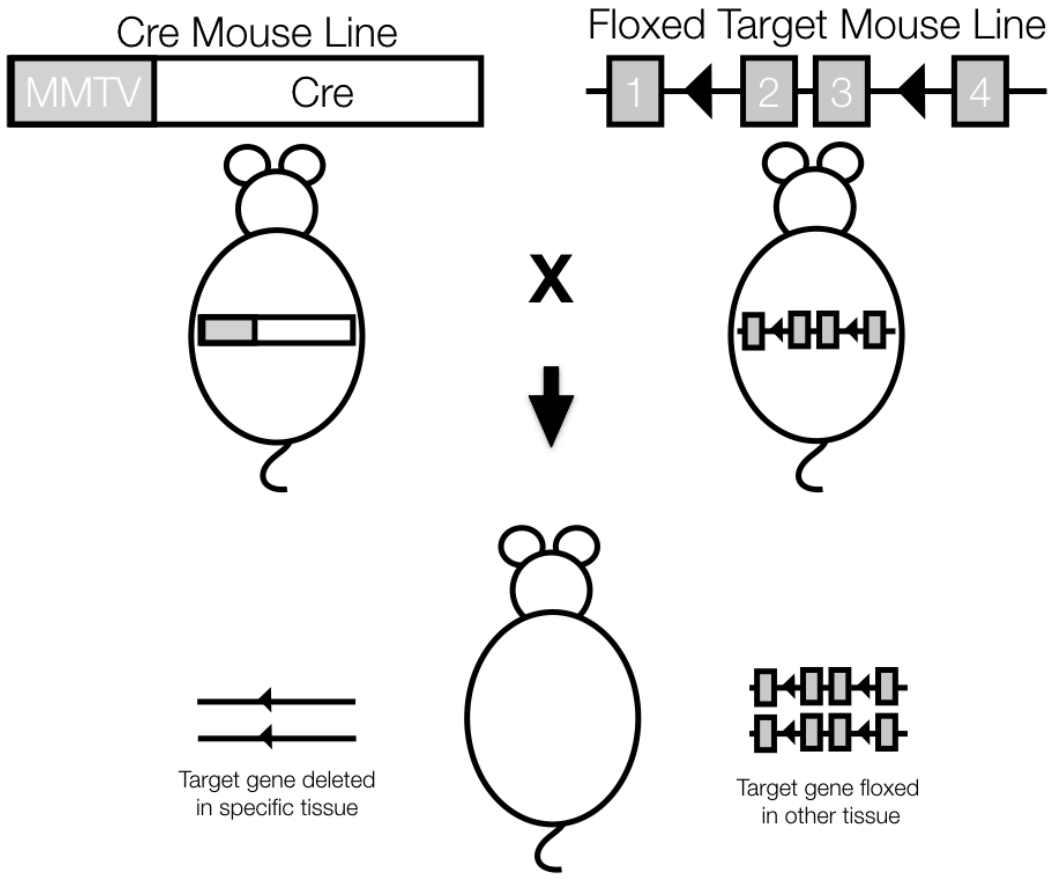
Cre Mouse Line
MMTV
Cre
Floxed Target Mouse Line
1
2
3
4
X
Target gene deleted
in specific tissue
Target gene floxed
in other tissue

B.

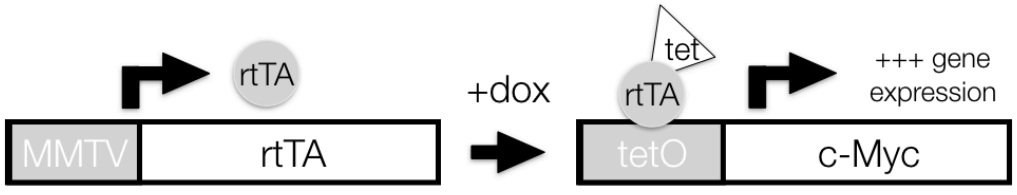
rtTA
MMTV
rtTA
+dox
tet
rtTA
tetO
c-Myc
+++ gene
expression

Figure 6. Overview of the Cre-loxP (A.) and MMTV-rtTA/ tetO-Myc (B.) systems used to create experimental GEM. To better determine the pathological relevance of BMI1 in c-Myc induced BC tumorigenesis we are creating a BMI1 knockout model. **(**A.) A Cre-loxP system will be utilized to result in a breast specific knockout of BMI1. Mice floxed in two of BMI1's introns ($BMI1^{loxp/loxp}$) will be crossed to transgenic mice with Cre expression under the mouse mammary tumor virus (MMTV-Cre). This will result in the cleavage of BMI1 in the breast tissue of mice progeny, with BMI1 expression remaining to be active in other tissues (B.) To promote BC tumorigenesis we are using a tetracycline system that drives c-Myc expression in the breast. We will be driving expression of reverse tetracycline controlled transactivator (rtTA) under the MMTV promoter. When in the presence of the tetracycline derivative, doxycycline (dox), tetracycline will bind rtTA and the resultant complex will bind the tetracycline inducible promoter (tetO), to result in increased transcription of gene expression of c-Myc in the breast.

Table 1. Mouse resources and generation numbers

Strain	**Original background**	**Source**	**Current generation number (N)**
MMTV-Cre	FVB x B6129F1	Jackson laboratories stock No. 003553	N6
MMTV- rtTA	C57BL/6 x SJL	Jackson Laboratories stock No. 010576	N4
tetO- Myc	FVB x B6129F1	Jackson Laboratories stock No. 019376	N5

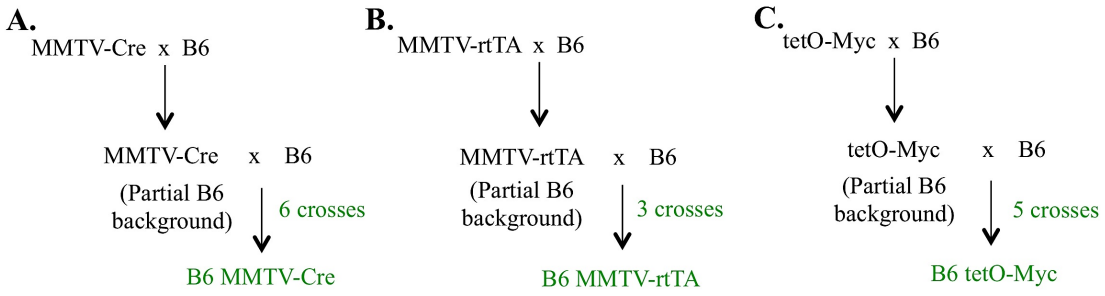
A.
MMTV-Cre x B6
MMTV-Cre x B6
(Partial B6 background)
6 crosses
B6 MMTV-Cre
B.
MMTV-rtTA x B6
MMTV-rtTA x B6
(Partial B6 background)
3 crosses
B6 MMTV-rtTA
C.
tetO-Myc x B6
tetO-Myc x B6
(Partial B6 background)
5 crosses
B6 tetO-Myc

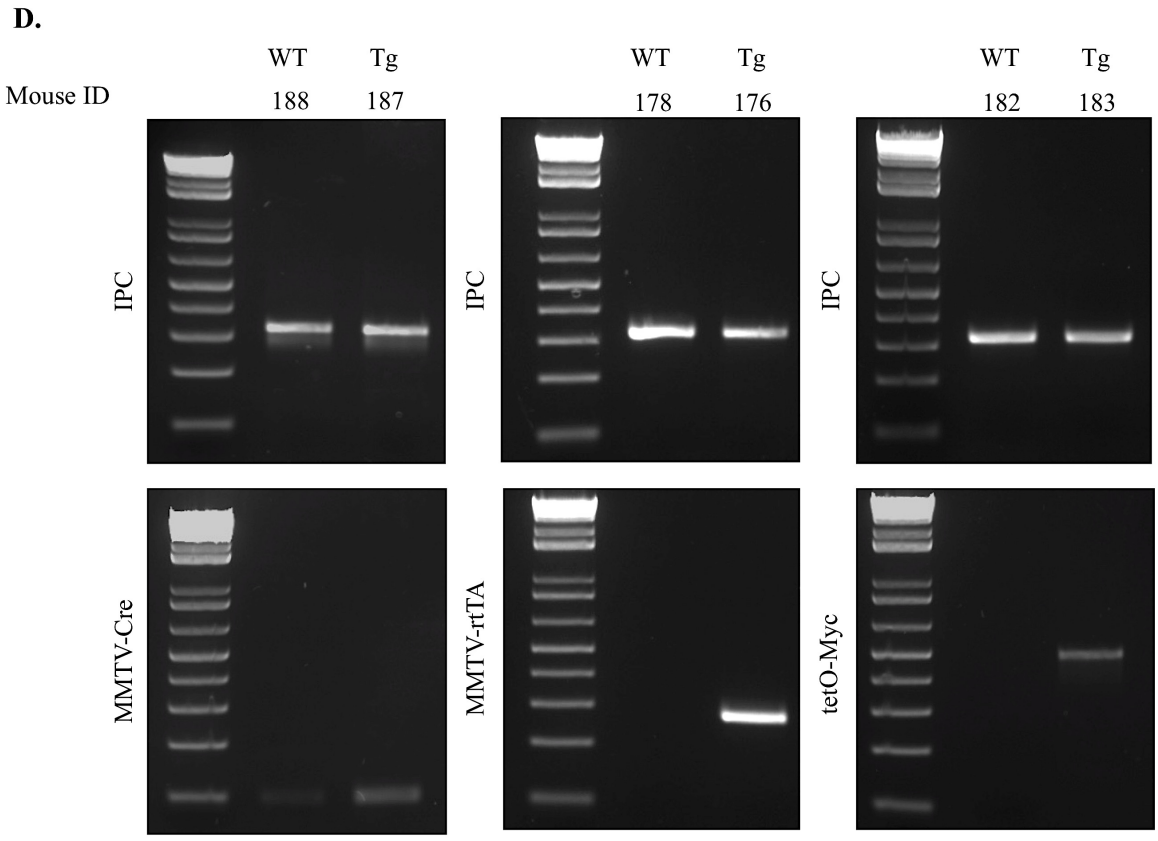
D.
Mouse ID
WT
Tg
188
187
178
176
182
183
IPC
MMTV-Cre
MMTV-rtTA
tetO-Myc

Figure 7. Backcrossing progress of the MMTV-Cre (A.), MMTV-rtTA (B.) and tetO-Myc (C.) transgenes into the C57BL/6 background and respective genotyping results (D.).

Male transgenic progeny were selected and crossed back to wildtype B6 females for 6 crosses (A.), 3 crosses (B.), and 5 crosses (C.) to reach true C57BL/6 congenicity. Genotyping of the MMTV-Cre (left panel), MMTV-rtTA (middle panel), and tetO-Myc (right panel) for the respective transgene proceeded every generation using ear genomic DNA and PCR techniques. WT: Wild type, Tg: Transgenic, IPC: Internal positive control. Every mouse is given a unique ID number as indicated. See Appendix I for detailed PCR components and conditions.

3.5 Transgenic line SNP testing

To determine the congenicity of the 3 transgenic mouse lines single nucleotide polymorphism (SNP) based genome screening is performed by Jackson Laboratories. SNP testing is run against three controls, B6J, SJL or FVB and Heterozygous (Het). The full report for all three transgenic lines supplied by Jackson Laboratories can be found in Appendix V.

MMTV-Cre and tetO-Myc were founded on mixed FVB x B6129F1 with a low percentage of original C57B/6 background expected. Due to the founding background the SNP panel was run against a FVB control. After 5 generations of backcrossing MMTV-Cre mouse samples ran to have approximately 98% (Sample 1: 97.93%; Sample 2: 98.29%) of wildtype C57BL/6 markers (Table 2). After 4 generations of backcrossing tetO-Myc mouse samples ran to have approximately 95% (Sample 1: 95.55%; Sample 2: 94.90%) of wildtype C57BL/6 markers (Table 3).

MMTV-rtTA was being stored in embryo and obtained through cryogenic recovery with a cross to SJL. This transgenic line was originally a C57BL/6 x SJL background but the supplier could not confirm the congenicity so transgenic N1 progeny tissue samples were sent for SNP testing. The SNP panel was run against a SJL control. When compared to wildtype C57BL/6 mice, our MMTV-rtTA N1 progeny ranged from having approximately 75% (Sample 1: 72.39%; Sample 2: 77.82%) of the wildtype C57BL/6 markers (Table 4).

Table 2. MMTV-Cre SNP based genome- screening results

	FVB	**C57BL/6J**
1	2.07%	97.93%
2	1.71%	98.29%
B6J	0.00%	100.00%
SJL	100.00%	0.00%
Het	50.00%	50.00%

Table 3. tetO-Myc SNP based genome- screening results

	FVB	**C57BL/6J**
1	4.45%	95.55%
2	5.10%	94.90%
B6J	0.00%	100.00%
SJL	100.00%	0.00%
Het	50.00%	50.00%

Table 4. MMTV-rtTA SNP based genome-screening results

	SJL	**C57BL/6J**
1	27.61%	72.39%
2	22.18%	77.82%
B6J	0.00%	100.00%
SJL	100.00%	0.00%
Het	50.00%	50.00%

CHAPTER 4: DISCUSSION AND FUTURE DIRECTIONS

Breast cancer remains a leading cause of cancer death in Canadian women; the disease is complex with much still yet to be elucidated. In general, BC is formed as a result of anti-tumor barriers being neutralized by continuous oncogenic insults or oncogene activation. It is thus essential to gain better insight into how BC tumorigenesis overcomes anti-tumor barriers. This knowledge will not only advance our understanding of BC but needs to be explored to improve BC diagnosis and therapy.

One integral anti-tumor barrier is the surveillance of abnormal cell proliferation, which is a result of elevated oncogene activation. An increase in cell proliferation is associated with replication stress and abnormalities in cell metabolisms; these collectively cause DNA damage, resulting in activation of the ATM-mediated DNA damage response (DDR) pathway. ATM causes cell cycle arrest, thereby inhibiting cell proliferation. It is a consensus that the ATM-derived anti-tumor barrier needs to be inactivated in order for BC tumorigenesis and progression. However, the mechanisms underlying ATM inactivation during tumorigenesis in general are unclear.

5.1 Exploration of BMI1's role in facilitation of c-Myc-induced BC using xenograft tumor models

My research provides initial evidence supporting the involvement of BMI1 in this process (see Introduction for detailed rationale). Briefly, we observed a reduction in γH2AX

levels in MCF7 cells that ectopically expressed both c-Myc and BMI1 when in comparison to MCF7 cells with ectopic expression of only c-Myc. Additionally it was found that the RF and HT BMI1 domains are not essential to this activity. My research is thus consistent with our recent publications reporting that BMI1 attenuates ATM activity through its association with NBS1 and that the RF motif, which is required for BMI1 to stimulate ubiquitin E3-ligase activity, is not required.

Although there is no significant difference in γH2AX foci formation between MCF7 EV and MCF7 BMI1 xenografts there is a trend of a smaller proportion of γH2AX foci levels in MCF7 BMI1 derived xenograft tumors. It is of further interest to see if γH2AX foci levels correlate with tissue sections proliferating at a different rate in these tumor sections. We hope to establish methods to further study the complex microenvironment found in MCF7 BMI1 expressing xenograft tumors to elucidate if BMI1- induced ATM inactivation, as seen through γH2AX levels, correspond with a higher proliferation rate of cells. γH2AX foci are a direct result of ATM activation and are a marker of DSB induced checkpoint activation, and BMI1 expression is established to decrease γH2AX foci levels in vitro. Thus it is possible that BMI1 expression may allow for accelerated cell proliferation through bypassing ATM-mediated checkpoint activation.

Collectively, my research has built a solid framework to further investigate the connection of BMI1 and attenuation of the ATM pathway during c-Myc-initiated BC tumorigenesis. Future work will need to focus on the functionality and mechanism behind

this association. With a set of BMI1 deletion mutants with individually missing important motifs, we are currently creating appropriate stable lines in MCF7 cells through retroviral infection expressing BMI1 or one of the four domain deletion mutants BMI1ΔRF, BMI1ΔHT, BMI1ΔPEST, and BMI1ΔNLS in conjunction with c-Myc. These stable lines will be analyzed for tumorigenesis in immunocompromised mice through either a subcutaneous (s.c.) route or an orthotopic model via mammary fat injection. It is expected that in comparison to c-Myc, MCF7 cells with co-expression of c-Myc and BMI1 or one of the deletion mutants will display elevations in tumorigenesis together with reductions in γH2AX and ATM activation, which can be detected using ATM serine 1981 phosphorylation.

The mammary orthotopic model has proven to be more advantageous compared to the s.c. model, with respect to the environment being more proper to breast cancer formation. Additionally, the orthotopic model can be used to examine BC metastasis, a critical step of cancer evolution, while most s.c. tumors do not progress to metastasis. Nonetheless, the s.c. model has its own advantages in that it is less invasive and more straightforward. Therefore the inclusion of both a s.c. and the orthotopic tumor model will enable a comprehensive analysis of the impact of BMI1 on c-Myc-derived breast cancer tumorigenesis and metastasis. Additionally we could also examine the effects of BMI1 on c-Myc-induced metastasis through tail vein delivery of MCF7 cells expressing c-Myc with and without co-expression of BMI1 or its deletion mutants.

5.2 Exploration of BMI1's role in facilitation of c-Myc-induced BC using Genetically Engineered Mouse (GEM) Models

To thoroughly investigate BMI1's collaboration with c-Myc during BC formation GEM need to be produced with a breast specific BMI1 deficiency and c-Myc transgenic expression. It has been established that a breast specific expression of c-Myc can be achieved using a combination of tetO-Myc and MMTV-rtTA transgenic mice on one common mouse line, and that this resultant transgenic expression leads to BC tumorigenesis (107). Compared to wildtype mice, *Myc* mice should result in the production of BC tumors with an upregulation of BMI1 and increased ATM activation. This is in line with our hypothesis that c-Myc transactivates BMI1 to facilitate oncogenic function through attenuation of ATM activity. Utilizing the tetO-Myc/MMTV-rtTA system in conjunction with a breast specific Cre- loxP knockout of BMI1 can create a *Cre;rtTA;Myc;BMI1*$^{-/-}$ GEM model that will allow for the de novo studying of breast tumorigenesis. Compared to wildtype mice it is predicted that *Cre;rtTA;Myc;BMI1*$^{-/-}$ GEM will have substantially increased ATM activation and reduced or delayed BC formation. This may also result in a decrease in cell proliferation index and a tumor environment more similar to control tumors since BMI1 is no longer present and able to inhibit ATM mediated checkpoint activation.

Before experimental crosses can proceed to create *Cre;rtTA;Myc;BMI1*$^{-/-}$ GEM, backcrossing of transgenic mouse lines on to a C57BL/6 congenic background needs to occur as phenotypic differences can result in resulting variation. Backcrossing is a very

involved process that is limited by the gestational cycle of the mouse. Speed congenic processes can be used that involves testing approximately 20 progeny every generation but is very expensive. It is integral for this process to stay consistent and timely so that experimental crosses can occur as soon as possible. Backcrossing of the three transgenic lines MMTV-Cre, tetO-Myc, and MMTV-rtTA on to a congenic C57BL/6 background is needed as the $BMI1^{loxp/loxp}$ mouse line was founded on this background (Table .1). A background percentage of over 95% C57BL/6 background is taken as congenic and is the suggested parameter set by Jackson Laboratories for all mouse lines. Single nucleotide polymorphism (SNP) genome based screening performed by Jackson Laboratories has been utilized to test the C57BL/6 background percentage for MMTV-Cre, tetO-Myc, and MMTV-rtTA at their N5, N4, and N1 generations respectively. The SNP results have shown that the C57BL/6 percentage for the MMTV- Cre (98%) and tetO-Myc (95%) lines are now above the threshold needed for experimental crosses to proceed. Since we are on the N4 backcross for MMTV-rtTA, with the N1 generation being on average 75% C57BL/6, it is anticipated that this is the last generation needed to reach congenicity (Table. 2).

With the completion of the three transgenic mouse strains MMTV-Cre, MMTV-rtTA, and tetO- Myc being transferred on to a congenic C57BL/6 background, intermediate lines (Figure 8A-C) will be generated to increase the rate of producing experimental Cre;rtTA;Myc;$BMI1^{-/-}$ mice (Figure 9). Similar strategies have been shown to be successful in maintaining Cre; $BMI1^{loxp/loxp}$ mice as MMTV- Cre should not be expressed

in males and c-Myc expression will be induced through administration of doxycycline (2 mg/ml) in drinking water. Mice will be monitored twice per week for tumor formation. Tumor volumes will be measured with calipers weekly for volume measurements until endpoint is reached (V= 1000 mm^3).

This model is not without its limitations. One possible downfall to this model is it involving an incomplete knockout of BMI1 due to the MMTV- Cre expression pattern. Although BMI1 is ubiquitously expressed in the mouse breast (111), MMTV-Cre expression is isolated to the luminal epithelial cells with a small population of these cells showing no expression of Cre (112, 113). Due to this there will be an incomplete knockout of BMI1 in this tissue**.** This incomplete MMTV-Cre expression may allow for an escapee cell population that can promote Myc powered tumorigenesis. To evaluate this possibility we aim to determine whether any tumors isolated

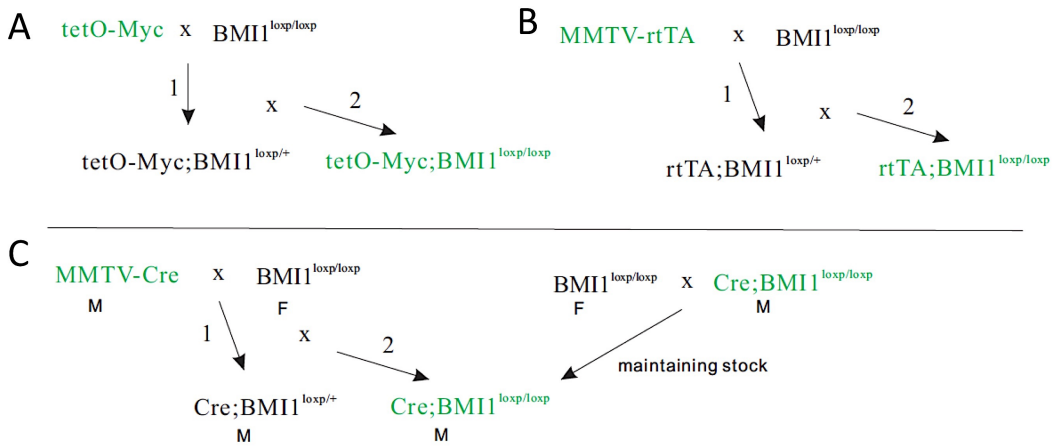

Figure 8. Plans to construct intermediate mouse lines. (A, B) Generation of the indicated lines will be performed to obtain homozygous mice for both transgenes. Lines will be maintained through crossing with C57BL/6 females. (C) Generation and maintenance of Cre; BMI1$^{loxp/loxp}$ will take advantage of MMTV-Cre not being expressed in males. This will additionally produce female BMI1$^{-/-}$ for experiments.

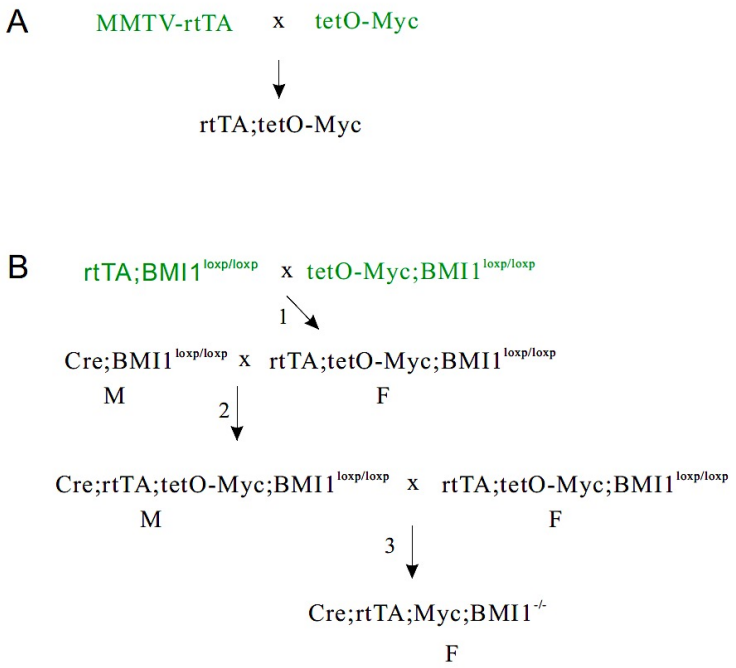

Figure 9. Creation of rtTA;tetO-Myc and Cre;rtTA;Myc;BMI1-/- mice. (A) Production of breast specific c-Myc mice (rtTA;tetO-Myc), with c-Myc expression induced upon addition of doxycycline to drinking water of females. (B) Plans to produce Cre;rtTA;Myc;BMI1$^{-/-}$ mice using intermediate lines generated in Figure 1A-C.

from *Myc;BMI1*$^{-/-}$ are derived from this escapee population though IHC staining as they would be Cre- negative, BMI1- positive, and Myc- positive.

BMI1 is known to inhibit the INK4-ARF locus that encodes p16^{INK4A} and p19/14^{ARF}, both being tightly involved in growth arrest, senescence, and apoptosis (73, 74). This provides another possible limitation as possible reduced or delayed BC formation may be contributed to by the reactivation of this locus. BMI1 mediated E3- Ub ligase activity is responsible for this interaction, so the impact of BMI1ΔRF in promoting c-Myc induced tumors will provide support that this activity is separate to INK4- ARF repression. To examine the importance of BMI1- derived inhibition of ATM activation in BC tumorigenesis, ATM inhibitor KU55933 will be utilized to further provide evidence that BMI1 facilitates BC tumorigenesis through directly inhibiting ATM. This is in line with it being reported that ATM activation causes a significant regression of Myc induced B-cell leukemia and that KU55933 enhances tumor load (114). In conjunction with this, the removal of doxycycline from the drinking water of *rtTA;tetO-Myc* causes a dramatic reduction in tumor load (107), and can be used to examine whether regression is reduced by KU5593.

5.3 Potential mechanisms of BMI1 mediated reduction of ATM activation in c-Myc-induced BC tumorigenesis

The xenografts and GEM tumors produced above can be used to investigate the mechanisms underlying BMI1-derived inhibition of ATM activation caused by c-Myc.

ATM activation is expected to reduce cell proliferation. We can examine this possibility by determining the index of cell proliferation using Ki67. We expect that tumors with co-expression of c-Myc and BMI1 will display increases in the proliferation index compared to the counterparts with only c-Myc overexpression. The contributions of the BMI1 domains to the enhancement of tumor cell proliferation can also be determined.

BC tumorigenesis and progression are a network process, in which multiple pathways will certainly be involved. The available set of tumors will be ideal to examine which pathways are mainly being affected. Gene expression can be profiled using either cDNA microarray or RNA sequencing in tumors produced by c-Myc activation and tumors with both c-Myc activation and BMI1 ectopic expression. This process will produce a set of differentially expressed genes (DEGs). The pathways affected by these DEGs can then be determined. Alternatively, profiling protein contents and modification can also be performed using mass spectrometry.

5.4 Clinical Implications

Clinically the finding that BMI1 attenuates oncogene induced ATM activation can direct how we may target BMI1 to suppress BC tumorigenesis development and progression. Developing an appropriate therapy to target BMI1 associated ATM attenuation needs to be specific to this process without affecting BMI1's role in other integral cellular function.

BMI1 has been established to be important for function of non-tumorigenic cells such as stem cell renewal and maintenance (63, 110). Complete knockout BMI1 mice are characterized by a survival rate of ~50% by the third day after birth with an increased frequency of illness, hematopoietic abnormalities in the liver and bone marrow, lymphoid abnormalities in the thymus and spleen, skeletal defects, ataxic gait, and reduced density in the cerebellum and neural layers (111), likely due to BMI1 expression being strongly expressed in embryonic stem cells during development to maintain axis specification and gene expression patterns (113). BMI1's role in stem cell maintenance has been attributed to its transcriptional repression of the INK4A-ARF locus mediated through BMI1's associated PRC1 E3- ub ligase activity (114). A downregulation of BMI1 activity through small molecule inhibitor therapy has been recently shown to suppress tumor growth and proliferation in a BC disease model (114).

One of the most significant conclusions from this data is that this activity is shown to be separate to known PRC1 E3- ub ligase activity, as seen by utilizing the BMI1ΔRF domain deletion mutant. Further elucidation of the specific mechanisms behind this association can allow for a more targeted approach to attenuating BMI1 that differentiates between BMI1- PRC1 function and its separate role in attenuating ATM activity. This specificity can be achieved at multiple levels. Future investigations may reveal the essential structural features contributing to BMI1's activity in reductions of oncogene-induced ATM activation. Small molecules can target these structures, with their presence possibly preventing BMI1 from inhibiting ATM activation. It can be envisaged that these

structural elements can be derived from BMI1, ATM, or other factors facilitating BMI1 to downregulate ATM activation. When investigating these structural elements in BMI1, a good starting point is to use BMI1 with deletion of both RF and HT. As deletion of neither was without effects on BMI1's activity in inhibiting ATM activation (judged on the levels of γH2AX) in MCF7 cells ectopically expressing c-Myc, it is possible that a double deletion mutant will also possess the full level activity. Using this deletion mutant, the structural motif essential for BMI1-derived activities in ATM inhibition can be mapped.

CHAPTER 5: CONCLUSIONS

The ATM-DDR pathway plays a critical role in inhibiting abnormal cell proliferation through proper cell cycle regulation. The reason this anti-tumor mechanism goes awry in breast tumorigenesis is not fully understood. This research aims to demonstrate a novel mechanism through which established oncogene, BMI1, may promote breast tumorigenesis independently of known PRC1 activity. We propose a novel activity in that BMI1 cooperates with oncogenes during BC formation to inhibit oncogene-induced ATM, thus promoting breast tumorigenesis.

The finding that ectopic expression of BMI1 in MCF7 BC cells inhibits oncogene-induced ATM activation supports this proposed role of BMI. Our work showing that the BMI1ΔRF deletion mutant lacking PRC1 E3- ubiquitin ligase function retains this function further suggests a novel role of BMI1 in inhibiting c-Myc induced ATM activation. Our manipulations of BMI1 and domain deletion mutants BMI1ΔRF, BMI1ΔHT, BMI1ΔPEST, and BMI1ΔNLS have helped further elucidate the specific mechanisms behind the collaboration of BMI1 and c-Myc in the attenuation of ATM activity. Although MCF7 BMI1 xenografts did not show a difference in ATM activation, as seen through γH2AX nuclear foci formation, both a more heterogeneous tumor environment indicative of a more aggressive tumor subtype, and a trend of a smaller proportion of cells positive for γH2AX nuclear foci in xenografts produced by MCF7 BMI1 was seen. Our development of a BMI1 *Cre;rtTA;Myc;BMI1*$^{-/-}$ GEM model will allow for the further studying of the pathological relevance of BMI1 in BC tumorigenesis.

Overall, we hope to better understand how BMI1 overcomes protective anti- tumor barriers through attenuation of ATM-mediated DDR. A better understanding of this pathway can help foster the development of clinical interventions aimed at counteracting DDR inactivation seen commonly in the formation of BC and other cancer types.

REFERENCES

1. Canadian Cancer Society's Advisory Committee on Cancer Statistics. Canadian Cancer Statistics 2017. Toronto, ON: Canadian Cancer Society; 2017. Available at: cancer.ca/Canadian-CancerStatistics-2017-EN.pdf.
2. Anders, C.K. *et al*. Young age at diagnosis correlates with worse prognosis and defines a subset of breast cancers with shared patterns of gene expression. *J. Clin. Oncol*. **20,** 3324–3330 (2008).
3. Collins, L.C. *et al*. Pathologic features and molecular phenotype by patient age in a large cohort of young women with breast cancer. *Breast Cancer Res.* **131,** 1061–1066 (2012).
4. Partridge, A.H. *et al*. The effect of age on delay in diagnosis and stage of breast cancer. *Oncologist*. **17,** 775–782 (2012).
5. Holford, T.R. *et al*. Changing patterns in breast cancer incidence trends. *J. Natl. Cancer. Inst. Monogr.* **36,** 19–25 (2006).
6. Berry, D.A. *et al*. Effect of screening and adjuvant therapy on mortality from breast cancer. *N. Engl. J. Med.* **353,** 1784-1792 (2005).
7. Fouad, Y. A. and Aanei, C. Revisiting the hallmarks of cancer. *Am. J. Cancer. Res*, **7,** 1016-1036 (2017).
8. Ojo, D. *et al.* Factors promoting tamoxifon resistance in breast cancer in stimulating breast cancer steam cell expansion. *Curr. Med. Chem.* **22,** 2360- 2374 (2015).
9. Ojo, D. *et al.* Polycomb complex protein BMI1 confers resistance to tamoxifen in estrogen receptor positive breast cancer. *Can. Letters.* **426,** 4-13 (2018).
10. Musgrove, E.A. *et al.* Cyclin D as a therapeutic target in cancer. *Nat. Rev. Cancer.* **11,** 558-572 (2011).
11. Arteaga, C.L. *et al.* Treatment of HER2- positive breast cancer: current status and future perspectives. *Nat. Rev. Clin. Onc.* DOI 10.1038/nrclinonc.2011.177 0.1038/nrclinonc.2011.177 (2011).
12. Musgrove, E.A. and Sutherland, R.L. Biological determinants of endocrine

resistance in breast cancer, *Nat. Rev. Cancer.* **9,** 631-643 (2009).

13. Ojo, D, Seliman, M. and Tang, D. Signatures derived from increase in CHARPIN gene copy number are associated with poor prognosis in patients with breast cancer. *BBA clinical.* **8,** 56-65 (2017).
14. Reddy, J.P. *et al.* Defining the ATM-mediated barrier to tumorigenesis in somatic mammary cells following ErbB2 activation. *Proc. Natl. Acad. Sci*. **107**, 3728-3733 (2010).
15. Yao, Y. and Dai, W. Genomic instability and cancer. *J. Carcinog. Mutagen.* **5,** 1-17 (2014).
16. Blanpain, C. *et al*. DNA-Damage Response in Tissue-Specific and Cancer Stem Cells. *Cell.* **8,** 16-29 (2010)
17. Mitchell, J. R., Hoeijmakers, J.H.J. and Niedernhofer, L.J. Divide and conquer : nucleotide excision repair battles cancer and ageing. *Curr. Opin. in Cell Biol.* **15,** 232–240 (2003).
18. de Boer, J. and Hoeijmakers, J.H. Nucleotide excision repair and human syndromes. *Carcinogenesis.* **3,** 453- 460 (2000).
19. Lindahl, T. An N-Glycosidase from Escherichia coli that releases free uracil from DNA containing deaminated cytosine residues. *Proc. Nat. Acad. Sci.* **71**, 3649-3653 (1974).
20. Li, G.M. Mechanisms and functions of DNA mismatch repair. *Cell Research.* **18,** 85-98 (2008).
21. Rich, T., Allen, R.L. and Wyllie, A.H. Defying death after DNA damage. *Nature.* **407**, 777–783 (2000).
22. Khanna, K. and Jackson, S. DNA double- strand breaks: signalling, repair, and the cancer connection. *Nature Genetics*. **27**, 247- 254 (2001).
23. You, Z. *et al.* CtlP Links DNA Double- strand Break Sensing to Resection. *Mol. Cell.* **36,** 954–969 (2010).
24. Jackson, A.P. Sensing and repairing DNA double-strand breaks. *Carcinogenesis.* **5,** 687-696 (2002).

25. Zhou, B. and Elledge, S. The DNA damage response: putting checkpoints in perspective. *Nature*, **408**, 433-439 (2000).
26. Hirao, A. *et al.* DNA damage- induced activation of p53 by the checkpoint kinase Chk2. *Science*. **287**, 1824-1827 (2000).
27. Lin, A. *et al*. A novel aspect of tumorigenesis- BMI1 functions in regulating DNA damage response. *Biomolecules*. **34**, 3063- 3075 (2015).
28. Zou, L. and Elledge, S.J. Sensing DNA damage through atrip recognition of RPA-ssDNA complexes. *Science*. **300**, 1542–1548 (2003).
29. Matsuoka, S. *et al.* ATM and ATR Substrate Analysis Reveals Extensive Protein Networks Responsive to DNA Damage. *Science.* **316,** 1160–1167 (2007).
30. Smith, J. *et al*. The ATM-CHK2 and ATR-CHK1 pathways in DNA damage signaling and cancer. *Adv. Cancer. Res*. **108**, 73–112 (2010).
31. Lee, J. and Paull, T.T. Activation and regulation of ATM kinase activity in response to DNA double-strand breaks. *Oncogene.* **26,** 7741–7748 (2007).
32. Liu, Q. *et al*. Chk1 is an essential kinase that is regulated by Atr and required for the G2/M DNA damage checkpoint. *Genes and Develop*. **14**, 1448-1459 (2000).
33. Difilippantonio, S. *et al.* Role of Nbs1 in the activation of the Atm kinase revealed in humanized mouse models. *Nat. Cell Biol*. **7**, 675-685 (2005).
34. Zhang, X., Liu, F. and Wang, W. Two-phase dynamics of p53 in the DNA damage response. *Proc. Natl. Acad. Sci.* **108,** 8990- 8995 (2011).
35. Lavin, M. F. *et al.* ATM Activation and DNA Damage Response. *Cell Cycle.* **6,** 931- 942 (2007).
36. Price, B.D. and D'Andrea, A.D. Chromatin remodeling at DNA double-strand breaks. *Cell*. **152,** 1344–1354 (2013).
37. Spycher, C. *et al.* Constitutive phosphorylation of MDC1 physically links the Mre11-Rad50-Nbs1complex to damaged chromatin. *J. Cell Biol.* **181,** 227–240 (2008).
38. Chapman, J.R. and Jackson, S.P. Phospho-dependent interactions between NBS1 and MDC1 mediate chromatin retention of the Mrn complex at sites of DNA

damage. *EMBO Rep.* **9,** 795–801 (2008).

39. Stucki, M. *et al*. MDC1 directly binds phosphorylated histone H2AX to regulate cellular responses to DNA double-strand breaks. *Cell.* **123,** 1213–1226 (2005).
40. Chapman, J.R., Taylor, M.R. and Boulton, S.J. Playing the end game: DNA double-strand break repair pathway choice. *Mol Cell.* **47,** 497–510 (2012).
41. McKinnon, P. DNA repair deficiency and neurological disease. *Nat. Rev. Neurosci*. **10**, 100-112 (2011).
42. de Klein, A. *et al*. Targeted disruption of the cell-cycle checkpoint gene ATR leads to early embryonic lethality in mice. *Curr. Biol.* **10**, 479-482 (2000).
43. Wood, L. D. *et al*. The genomic landscapes of human breast and colorectal cancers. *Science*. **318,** 1108–1113 (2007).
44. Sarni, D. and Kerem, B. Oncogene-Induced Replication Stress Drives Genome Instability and Tumorigenesis. *Int. J. Mol. Sci.* **18,** 1-10 (2017).
45. Powers, J. T. *et al.* E2F1 Uses the ATM Signaling Pathway to Induce p53 and Chk2 Phosphorylation and Apoptosis. *Mol. Can. Res.* **2,** 203–214 (2004).
46. Gorgoulis, V. G. et al. Activation of the DNA damage Checkpoint and genomic instability in human precancerous lesions. *Nature*. **434,** 907–913 (2005).
47. Bartkova, J. et al. DNA damage response as a candidate anti-cancer barrier in early human tumorigenesis. *Nature*. **434,** 864–870 (2005).
48. Halazonetis, T.D., Gorgoulis, V.G. and Bartek, J. An oncogene-induced DNA damage model for cancer development. *Science.* **319,** 1352–1355 (2008).
49. Haupt, Y. *et al*. Novel zinc finger gene implicated as myc collaborator by retrovirally accelerated lymphomagenesis in E mu-myc transgenic mice. *Cell*. **65**, 753-763 (1991).
50. van Lohuizen, M. *et* al. Identification of cooperating oncogenes in E mu-myc transgenic mice by provirus tagging. *Cell*. **65**, 737-752 (1991).
51. Miller, A.M. *et al*. c-Myc and Cancer Metabolism. *Clin. Cancer Res.* **18,** 5546-5553 (2012).

52. Gearhart, J. *et al*. Pluripotency Redux- Advances in Stem- Cell Research. *New Engl. J. Med.* **357,** 1469- 1472 (2007).
53. Kim, J.H. *et al*. Overexpression of Bmi-1 oncoprotein correlates with axillary lymph node metastases in invasive ductal breast cancer. *Breast*. **13**, 383-388 (2004).
54. Guo, B.H. *et al*. Bmi-1 promotes invasion and metastasis, and its elevated expression is correlated with an advanced stage of breast cancer. *Molecular Cancer*. **10**, 10 (2011).
55. Bea, S. *et* al. BMI-1 gene amplification and overexpression in hematological malignancies occur mainly in mantle cell lymphomas. *Cancer Research*. **61**, 2409-2412 (2001).
56. van Galen, J.C. *et al*. Expression of the polycomb-group gene BMI1 is related to an unfavourable prognosis in primary nodal DLBCL. *J. Clin. Pathol*. **60,** 167-172 (2007).
57. Fan, C. *et al*. Bmi1 promotes prostate tumorigenesis via inhibiting p16(INK4A) and p14(ARF) expression. *Biochim. Biophys. Acta*. **1782,** 642-648 (2008).
58. Kim, J.H. *et al*. The Bmi-1 oncoprotein is overexpressed in human colorectal cancer and correlates with the reduced p16INK4a/p14ARF proteins. *Cancer Letters*. **203,** 217-224 (2004).
59. Gavrilescu, M.M. *et al*. Expression of bmi-1 protein in cervical, breast and ovarian cancer. *Rev. Med. Chir. Soc. Med. Nat. Iasi*. **116,** 1112-1117 (2012).
60. Leung, C. *et al.* Bmi1 is essential for cerebellar development and is overexpressed in human medulloblastomas. *Nature*. **428,** 337-341 (2004).
61. Huang, R. *et al*. MYCN and MYC regulate tumor proliferation and tumorigenesis directly through BMI1 in human neuroblastomas. *FASEB J.* **25**, 4138-4149 (2011).
62. Yang, M.H. *et al*. Bmi1 is essential in Twist1-induced epithelial-mesenchymal transition. *Nature Cell Biology*. **12,** 982-992 (2010).
63. Ma, J. *et al*. Characterization of mammary cancer stem cells in the MMTV-PyMT

mouse model. *Tumor Biol*. **33,** 1983-1996 (2012).

64. Dimri, G.P. *et al*. The Bmi-1 oncogene induces telomerase activity and immortalizes human mammary epithelial cells. *Cancer Research*. **62,** 4736-4745 (2002).
65. Waldron, T. *et* al. c-Myb and its target Bmi1 are required for p190BCR/ABL leukemogenesis in mouse and human cells. *Leukemia*. **26,** 644-653 (2012).
66. Cao, R., Tsukada, Y. and Zhang, Y. Role of Bmi-1 and Ring1A in H2A ubiquitylation and Hox gene silencing. *Molecular cell*. **20,** 845-854 (2005).
67. Pherson, M. *et al.* Polycomb repressive complex 1 modifies transcription of active genes. *Sci. Adv.* **2,** 1–17 (2017).
68. Wang, H., Wang, L. and Erdjument-bromage, H. Role of histone H2A ubiquitination in Polycomb silencing. *Nature.* **431,** 873–878 (2004).
69. Li, Z. *et* al. Structure of a Bmi-1-Ring1B polycomb group ubiquitin ligase complex. *J. Biol. Chem.* **281,** 20643-20649 (2006).
70. Ismail, H. *et al*. J. BMI1-mediated histone ubiquitylation promotes DNA double-strand break repair. *J. Cell Biol.* **191,** 45–60 (2010).
71. Chagraoui, J. *et al*. An anticlastogenic function for the polycombgroup gene BMI1. *Proc. Natl. Acad. Sci*. **108,** 5284–5289 (2011).
72. Molofsky, A.V. *et al*. Bmi-1 promotes neural stem cell self-renewal and neural but not mouse growth and survival by repressing the p16Ink4a and p19Arf senescence pathways. *Genes Dev.* **19,** 1432-1437 (2005).
73. Chin, L., Pomerantz, J. and DePinho, R.A. The INK4a/ARF tumor suppressor: one gene--two products--two pathways. *Trends Biochem. Sci*. **23,** 291-296 (1998).
74. Sherr, C.J. Tumor surveillance via the ARF-p53 pathway. *Genes Dev*. **12,** 2984-2991 (1998).
75. Levine, A. J. p53 , the Cellular Gatekeeper for Growth and Division. *Cell.* **88,** 323–331 (1997).
76. Bruggeman, S.W. *et al*. Ink4a and Arf differentially affect cell proliferation and neural stem cell self-renewal in Bmi1-deficient mice. *Genes Dev.* **19,** 1438-1443

(2005).

77. Cohen, K.J. *et* al. Transformation by the Bmi-1 oncoprotein correlates with its subnuclear localization but not its transcriptional suppression activity. *Mol. Cell. Biol.* **16,** 5527-5535 (1996).

78. Dong, Q. *et al*.. Radioprotective effects of BMI-1 involve epigenetic silencing of oxidase genes and enhanced DNA repair in normal human keratinocytes. *J. Investig. Dermatol.* **131,** 1216–1225 (2011).

79. Wang, E. *et* al. Enhancing chemotherapy response with BMI-1 silencing in ovarian cancer. *PLOS ONE* **6,** doi:10.1371/journal.pone.0017918 (2011).

80. Wei, F. *et al*. BMI1 attenuates etoposide-induced G2/M checkpoints via reducing ATM activation. *Oncogene*. **34**, 3063-3075 (2015).

81. Williams, G.J., Lees-Miller, S.P. and Tainer, J.A. Mre11-Rad50-Nbs1 conformations and the control of sensing, signaling, and effector responses at DNA double-strand breaks. *DNA Repair*. **9**, 1299–1306 (2010).

82. Li, Z., Cao, R., Wang, M., Myers, M.P., Zhang, Y. and Xu, R.M. (2006) Structure of a Bmi-1-Ring1B polycomb group ubiquitin ligase complex. *J. Biol. Chem.* **281**, 20643-20649.

83. Lloyd, J. *et al*. A supramodular FHA/BRCT-repeat architecture mediates NBS1 adaptor function in response to DNA damage. *Cell.* **139,** 100–111 (2009).

84. Becker, E. *et al*. Detection of a tandem BRCT in NBS1 andXRS2 with functional implications in the DNA damage response. *Bioinformatics.* **22,** 1289–1292 (2006).

85. Lee, J.H. and Paull, T.T. Activation and regulation of ATM kinase activity in response to DNA double-strand breaks. *Oncogene.* **26,** 7741–7748 (2007).

86. Desai-Mehta, A., Cerosaletti, K.M. and Concannon, P. Distinct functional domains of nibrin mediate Mre11 binding, focus formation, and nuclear localization. *Mol. Cell. Biol.* **21,** 2184–2191 (2001).

87. Falck, J., Coates, J. and Jackson, S.P. Conserved modes of recruitment of ATM, ATR and DNA-PKcs to sites of DNA damage. *Nature*. **434,** 605–611 (2005).

88. Huang, R. *et al*. Mycn and myc regulate tumor proliferation and tumorigenesis

directly through BMI1 in human neuroblastomas. *FASEB J*. **25,** 4138–4149 (2011).

89. Waldron, T. *et al*. c-Myb and its target Bmi1 are required for p190BCR/ABl leukemogenesis in mouse and human cells. *Leukemia*. 26, 644–653 (2012).
90. Wang, H.B. *et al*. SP1 and c-Myc regulate transcription of Bmi1 in nasopharyngeal carcinoma. *FEBS J*. **280,** 2929–2944 (2013).
91. Datta, S. *et al. Bmi*-1 cooperates with H-Ras to transform human mammary epithelial cells via dysregulation of multiple growth-regulatory pathways. *Cancer Res*. **67**, 10286-10295 (2007).
92. Tatrai, P. *et al.* Combined introduction of Bmi-1 and hTERT immortalizes human adipose tissue-derived stromal cells with low risk of transformation. *Biochem. Biophys. Res. Comm*. **422**, 28-35 (2012).
93. Jacobs, J.J. *et al.* Bmi-1 collaborates with c-Myc in tumorigenesis by inhibiting c-Myc-induced apoptosis via INK4a/ARF. *Genes Dev.* **13,** 2678–2690 (1999).
94. Goldgar, D.E. *et al.* Rare variants in the ATM gene and risk of breast cancer. *Breast Cancer Res*. **13**, doi: 10.1186/bcr2919 (2011).
95. Hoenerhoff, M.J. *et al.* BMI1 cooperates with H-RAS to induce an aggressive breast cancer phenotype with brain metastases. *Oncogene*. **28**, 3022-3032 (2009).
96. Walrath, J.C. *et al* Genetically engineered mouse models in cancer research. *Adv. Cancer Res.* **106,** 113- 164 (2010).
97. Blyth, K., Morton, J. P. and Sansom, O. J. The right time, the right place: will targeting human cancer-associated mutations to the mouse provide the perfect preclinical model? *Curr. Opin. Genet. Dev.* **22,** 28-35 (2012).
98. Holen, I., *et al.* In vivo models in breast cancer research: progress, challenges and future directions. *Dis. Models Mech.* **10,** 357-371 (2017).
99. Sorlie, T., *et al.* Repeated observation of breast tumor subtypes in independent gene expression data sets. *Proc. Natl. Acad. Sci.* **100,** 8418-8423 (2003).
100. Whittle, J. R. *et al.* Patient derived xenograft models of breast cancer and their predictive power. *Breast Cancer Res*. **17,** 17 (2015).

101. Sinn, E. *et al.* Coexpression of MMTV/v-Ha-ras and MMTV/c-Myc genes in transgenic mice: synergistic action of oncogenes in vivo. *Cell.* **49,** 465 – 475 (1987).

102. Jonkers, J. and Berns, A. Conditional mouse models of sporadic cancer. *Nat. Rev. Cancer.* **2,** 251 – 265 (2002).

103. Shibata, H. *et al*. Rapid colorectal adenoma formation initiated by conditional targeting of the Apc gene. *Science*. **278,** 120 – 123 (1997).

104. Frese, K.K. and Tuveson, D.A. Maximizing mouse cancer models. *Nat. Rev. Cancer.* **7,** 645 – 658 (2007).

105. Gossen, M. *et al.* Transcriptional activation by tetracyclines in mammalian cells. *Science.* **268,** 1766 – 1769 (1995).

106. Felsher, D.W. and Bishop, J.M. Reversible tumorigenesis by MYC in hematopoietic lineages. *Mol. Cell.* **4,** 199 – 207 (1999).

107. D'Cruz, C.M. *et al.* c-Myc induces mammary tumorigenesis by means of a preferred pathway involving spontaneous Kras2 mutations. *Nat. Med*. **7**, 235-239 (2001).

108. Kawamoto, S. *et al.* A novel reporter mouse strain that expresses enhanced green fluorescent protein upon Cre-mediated recombination. *FEBS Lett*. **470**, 263-268 (2000).

109. Maynard, M.A. *et al.* Bmi1 is required for tumorigenesis in a mouse model of intestinal cancer. *Oncogene.* **33,** 3742- 3747 (2014).

110. Yan, J., Tang, D. Prostate cancer stem- like cells proliferate slowly and resist etoposide induced cytotoxicity via enhancing DNA damage response. *Exp. Cell Res.* **328,** 132- 142 (2014).

111. Yan, K.S. *et al.* The intestinal stem cell markers BMI1 and Lgr5 identify two functionally distinct populations. *Proc. Natl. Acad. Sci.* **109,** 466- 471 (2012).

112. van der Lugt, N.M. *et al.* Posterior transformation, neurological abnormalities, and severe hematopoietic defects in mice with a targeted deletion of the bmi-1 proto-oncogene. *Genes Dev.* **8,** 757-769 (1994).

113. del Mar Lorente, M. *et al.* Loss-and gain-of-function mutations show a polycomb group function for Ring1A in mice. *Develop.* **127,** 5093- 5100 (2000).

114. Srinivasan, M. *et al.* Downregulation of Bmi1 in breast cancer stem cells suppresses tumor growth and proliferation. *Oncotarget*. **8,** 38731- 38742 (2017).

APPENDIX

Appendix I

MMTV-Cre PCR Components

Reaction Component	Final Concentration	Volume (ul)
HS Buffer (10x)	1x	1.2
$MgCl_2$ (50 mM)	2mM	0.48
dNTP (10 mM)	0.2 mM	0.24
FWD (10mM)	1 mM	1.2
RVS (10mM)	1 mM	1.2
Taq (5 U/ul)	0.01 U/ul	0.024
ddH_2O	\	6.7
DNA	0.25-0.5 ug/ul	0.5-1

TetO-Myc and MMYC-rtTA PCR Components

Reaction Component	Final Concentration	Volume (ul)
HS Buffer (10x)	1x	1.2
$MgCl_2$ (25 mM)	2mM	0.96
dNTP (10 mM)	0.2 mM	0.24
FWD (10mM)	0.5 mM	0.6
RVS (10mM)	0.5 mM	0.6
HS Taq (5 U/ul)	0.01 U/ul	0.024
ddH_2O	\	7.4
DNA	0.25-0.5 ug/ul	0.5-1

MMTV-Cre PCR Protocol

Step #	Temp °C	Time	Note
1	94	3 min	
2	94	30 sec	
3	51.7	1 min	
4	72	1 min	repeat steps 2-4 for 35 cycles
5	72	2 min	
6	10		hold

TetO-Myc and MMTv- rtTA PCR Protocol

Step #	Temp °C	Time	Note
1	94	2 min	
2	94	20sec	
3	65	15sec	-0.5 C per cycle decrease
4	68	45sec	
5			repeat steps 2-4 for 10 cycles
6	94	15sec	
7	60	15sec	
8	72	45sec	
9			repeat steps 6-8 for 28 cycles
10	72	2 min	
11	10		hold

Appendix II

Table 1. Descriptive statistics for % γH2AX levels of EV, BMI1, BMI1ΔRF

Group	N	Minimum	Maximum	Mean	Std. Error	Std. Deviation
EVEV	3	36.00	42.00	40.0000	2.00000	3.46410
EVCMYC	3	68.00	80.00	75.3333	3.71184	6.42910
EVBMI	3	38.00	48.00	43.3333	2.90593	5.03322
BMICMYC	3	40.00	46.00	44.0000	2.00000	3.46410
EVRF	3	38.00	46.00	42.0000	2.30940	4.00000
RFCMYC	3	40.00	48.00	44.0000	2.30940	4.00000

Table 2. Independent t-tests for % γH2AX levels of EV, BMI1, BMI1ΔRF

Group	t	df	Sig. (2-tailed)
EVEV / EVCMYC	-8.38	4	0.001
EVBMI1/ BMI1CMYC	-.189	4	0.859
EVRF/ RFCMYC	-.612	4	0.573
EVEV/ EVBMI1	-.945	4	0.398
EVEV/EVRF	-1.342	4	0.272
EVCMYC/ BMI1CMYC	7.431	4	0.002
EVCMYC/ RFCMYC	7.167	4	0.002

Appendix III

Table 1. Descriptives Statistics for % γH2AX levels of EV, BMI1ΔHT, BMI1ΔPEST, BMI1ΔNLS

Group	N	Minimum	Maximum	Mean	Std. Error	Std. Deviation
EVEV	3	38.00	42.00	40.6667	1.33333	2.30940
EVCMYC	3	68.00	70.00	68.6667	.66667	1.15470
EVHT	3	42.00	44.00	42.6667	.66667	1.15470
HTCMYC	3	36.00	44.00	39.3333	2.40370	4.16333
EVPEST	3	36.00	44.00	41.3333	2.66667	4.61880
PESTCMYC	3	54.00	58.00	56.6667	1.33333	2.30940
EVNLS	3	40.00	42.00	40.6667	.66667	1.15470
NLSCMYC	3	58.00	60.00	59.3333	.66667	1.15470

Table 2. Independent t-test statistics for % γH2AX levels of EV, BMI1ΔHT, BMI1ΔPEST, BMI1ΔNLS

Group	t	df	Sig. (2-tailed)
EVEV / EVCMYC	-18.783	4	0.000047
EVHT/ HTCMYC	1.336	4	0.252
EVPEST/ PESTCMYC	-5.143	4	0.007
EVNLS/ NLSCMYC	-19.799	4	0.000038
EVEV/ EVHT	-1.432	4	0.251
EVEV/EVPEST	-.224	4	.834
EVEV/ EVNLS	.148	4	1.000
EVCMYC/ HTCMYC	11.759	4	0.000299
EVCMYC/ PESTCMYC	8.050	4	0.001
EVCMYC/ NLSCMYC	9.899	4	0.001

Appendix IV

Table 1. Descriptive statistics for γH2AX nuclear foci levels for EV and BMI1 xenografts

Group	N	Minimum	Maximum	Mean	Std. Error	Std. Deviation
EV	3	8.70	17.67	13.2878	2.59390	4.49276
BMI1	3	9.09	15.35	11.9804	1.82135	3.15468

Table 2. Independent t-test for γH2AX nuclear foci levels for EV and BMI1 xenografts

Group	t	df	Sig. (2-tailed)
EV / BMI1	.412	4	.701

Appendix V

Table 1. Full SNP genome- screening results for MMTV- Cre mice.

			474202 3	474202 4	B6J	FVB	Het
SNP_ID	Expected SNPs						
Chromosome-bp	C57BL/6J	FVB/NJ	1	2	B05	B07	B09
01-010053195-M	G	T	G	G	G	T	T/G
01-031264126-M	C	T	C	C	C	T	T/C
01-047362047-M	T	C	T	T	T	C	C/T
01-067230857-N	G	T	G	G	G	T	G/T
01-080181487-M	T	A	T	T	T	A	A/T
01-106073928-M	T	C	T	T	T	C	C/T
01-126055046-M	A	T	A	A	A	T	T/A
01-139952425-M	A	T	A	A	A	T	T/A
01-150718101-M	T	C	T	T	T	C	C/T
01-180301121-G	C	T	C	C	C	T	T/C
01-194803746-N	G	T	G	G	G	T	T/G
02-031721080-G	A	G	A	A	A	G	A/G
02-047368792-G	T	C	T	T	T	C	T/C
02-063356615-N	G	A	G	G	G	A	A/G
02-072065558-N	G	T	G	G	G	T	T/G
02-094964773-M	G	T	G	G	G	T	T/G
02-114758266-N	T	C	T	T	T	C	C/T
02-131136658-M	C	A	C	C	C	A	A/C
02-159897340-M	G	A	G	G	G	A	A/G
02-172504164-G	C	T	C	C	C	T	T/C
03-007561998-N	T	C	T	T	T	C	C/T
03-022347144-G	T	C	T	T	T	C	C/T
03-035115028-M	C	T	C	C	C	T	T/C
03-056067960-G	T	C	T	T	T	C	T/C
03-075336142-M	A	G	A	A	A	G	G/A
03-095186319-G	C	A	C	C	C	A	C/A
03-115468851-N	C	A	C	C	C	A	A/C
03-131286062-N	C	T	C	C	C	T	C/T

03-151125653-M	A	T	A	A	A	T	T/A
04-006370062-M	A	G	A	A	A	G	G/A
04-017015246-M	T	C	T	T	T	C	C/T
04-034965128-M	A	C	A	A	A	C	C/A
04-053894587-M	T	C	T	T	T	C	C/T
04-068252469-M	C	T	C	C	C	T	T/C
04-097015585-M	A	G	A	A	A	G	G/A
04-117567852-N	C	T	C	C	C	T	T/C
04-128694339-G	T	G	T	T	T	G	T/G
04-142807236-G	G	A	G	G	G	A	A/G
05-013136419-M	C	T	C	C	C	T	T/C
05-035182717-N	T	G	T	T	T	G	G/T
05-041667588-G	G	T	G	G	G	T	T/G
05-061148036-G	T	C	T	T	T	C	T/C
05-076427870-N	A	G	A	A	A	G	G/A
05-118031699-M	G	A	G	G	G	A	A/G
05-145143884-M	C	T	C	C	C	T	T/C
06-011983883-M	G	C	C/G	C/G	G	C	C/G
06-023207025-M	A	G	A	A	A	G	G/A
06-038230055-G	A	G	A	A	A	G	G/A
06-048811360-N	G	T	G	G	G	T	T/G
06-076285738-M	T	A	T	T	T	A	A/T
06-090142535-M	C	A	A/C	A/C	C	A	A/C
06-112199886-M	G	T	T/G	T/G	G	T	T/G
06-126258422-M	T	C	C/T	C/T	T	C	C/T
07-034063244-M	G	A	G	G	G	A	A/G
07-053928010-M	T	G	T	T	T	G	G/T
07-064095712-M	G	T	G	G	G	T	T/G
07-082671949-N	C	G	C	C	C	G	G/C
07-094312514-M	A	G	A	A	A	G	G/A
07-112553982-G	T	G	T	T	T	G	T/G
07-124000818-G	T	C	T	T	T	C	T/C
08-015199792-M	T	C	T	T	T	C	C/T
08-032490228-N	A	G	A	A	A	G	G/A
08-053200795-M	T	C	T	T	T	C	C/T
08-065849115-N	A	G	A	A	A	G	G/A
08-088063837-N	C	T	C	C	C	T	T/C
08-101099186-M	A	T	A	A	A	T	T/A

08-117163724-M	G	A		G	G	A	A/G
09-017770060-M	T	A	T	T	T	A	A/T
09-029233439-N	A	G	A	A	A	G	A/G
09-037841497-M	T	C	T	T	T	C	C/T
09-063923771-M	G	A	G	G	G	A	A/G
09-084055613-M	C	A	C	C	C	A	A/C
10-008017793-M	A	C	A	A	A	C	C/A
10-028554348-N	G	A	G	G	G	A	G/A
10-053898997-M	G	C	G	G	G	C	C/G
10-060074134-G	G	A	A/G	A/G	G	A	A/G
10-077371167-G	G	A	G	G	G	A	A/G
10-099683776-N	C	G	C	C	C	G	G/C
10-120289167-M	A	G	A	A	A	G	G/A
11-004367508-M	G	A	G	G	G	A	A/G
11-022864828-N	C	A	C	C	C	A	A/C
11-033040833-M	T	C	T	T	T	C	C/T
11-061500282-N	T	C	T	T	T	C	C/T
11-077198334-M	G	A	G	G	G	A	A/G
11-098391535-G	T	G	T	T	T	G	G/T
11-113224684-M	A	G	A	A	A	G	G/A
12-009581325-M	G	T	G	G	G	T	T/G
12-031510473-N	G	A	G	G	G	A	A/G
12-049281625-M	C	T	C	C	C	T	T/C
12-064212930-N	A	G	A	A	A	G	A/G
12-106729531-M	T	C	T	T	T	C	C/T
13-011923617-M	T	C	T	T	T	C	C/T
13-026482435-G	A	G	A	A	A	G	G/A
13-037832161-M	A	T	A	A	A	T	T/A
13-059590161-N	C	T	C	C	C	T	T/C
13-078326044-G	C	T	C	C	C	T	T/C
13-085133616-G	T	C	T	T	T	C	T/C
13-093046894-N	C	T	C	C	C	T	T/C
13-110566702-N	C	T	C	C	C	T	T/C
13-112696462-N	A	C	A	A	A	C	C/A
14-005055006-M	T	A	T	T	T	A	A/T
14-022368155-G	T	C	T	T	T	C	T/C
14-033881274-G	A	T		A	A	T	T/A
14-055918382-M	C	T	C	C	C	T	T/C

14-079218045-M	C	A	C	C	C	A	A/C
14-095233920-G	T	C	T	T	T	C	T/C
14-110887447-M	C	T	C	C	C	T	T/C
15-005994001-M	A	C	A	A	A	C	C/A
15-028279166-G	T	C	T	T	T	C	T/C
15-041919640-N	C	T	C	C	C	T	T/C
15-055206736-N	G	A	G	G	G	A	A/G
15-069647296-G	T	G	T	T	T	G	G/T
15-087100507-M	A	G	A	A	A	G	G/A
15-096231715-M	T	G	T	T	T	G	G/T
16-003310511-N	G	A	G	G	G	A	A/G
16-019621494-C	A	G	A	A	A	G	A/G
16-035239412-C	C	G	C	C	C	G	C/G
16-051080938-C	A	T	A	A	A	T	T/A
16-068107787-C	G	A	G	G	G	A	A/G
16-093066825-C	T	C	T	T	T	C	T/C
17-007230139-M	C	G	C	C	C	G	G/C
17-028172639-M	C	T	C	C	C	T	T/C
17-037829090-G	G	T	G	G	G	T	G/T
17-056073815-M	G	A	G	G	G	A	A/G
17-065004394-N	T	C	T	T	T	C	C/T
17-082297869-M	T	G	T	T	T	G	G/T
17-092673068-N	T	G	T	T	T	G	T/G
18-010953833-N	A	G	A	A	A	G	A/G
18-029963387-M	T	C	T	T	T	C	C/T
18-055728214-N	G	C	G		G	C	C/G
18-075088655-M	G	A	G	G	G	A	A/G
18-086980249-M	G	A	G	G	G	A	A/G
19-003607482-N	C	T	T/C	C	C	T	T/C
19-013339654-M	A	C	A	A	A	C	C/A
19-034003337-G	G	T	G	G	G	T	T/G
19-046168493-M	G	A	G	G	G	A	A/G
19-060030696-N	A	G	A	A	A	G	G/A
X-016114535-G	C	A	C	C	C	A	A/C
X-022427259-G	C	A	C	C	C	A	C/A
X-034968801-G	G	A	G	G	G	A	A/G
X-042691780-G	T	A	T	T	T	A	T/A
X-054650362-N	T	A	T	T	T	A	A/T

X-074884405-G	A	G	A	A	A	G	A/G
X-087817653-G	A	T	A	A	A	T	T/A
X-109677875-M	A	G	A	A	A	G	G/A
X-123551831-M	A	G	A	A	A	G	G/A
X-143466659-M	A	C	A	A	A	C	C/A

Table 2. Full SNP genome- screening results for tetO-Myc mice.

			1	2	B6J	FVB	Het
SNP_ID	Expected SNPs						
Chromosome-bp	C57BL/6J	FVB/NJ	1	2	B05	B07	B09
01-010053195-M	G	T	G	G	G	T	T/G
01-031264126-M	C	T	C	C	C	T	T/C
01-047362047-M	T	C	T	T	T	C	C/T
01-067230857-N	G	T	G	G	G	T	G/T
01-080181487-M	T	A	T	T	T	A	A/T
01-106073928-M	T	C	T	T	T	C	C/T
01-126055046-M	A	T	A	A	A	T	T/A
01-139952425-M	A	T	A	A	A	T	T/A
01-150718101-M	T	C	T	T	T	C	C/T
01-180301121-G	C	T	C	C	C	T	T/C
01-194803746-N	G	T	G	G	G	T	T/G
02-031721080-G	A	G	A	A	A	G	A/G
02-047368792-G	T	C	T/C	T	T	C	T/C
02-063356615-N	G	A	G	G	G	A	A/G
02-072065558-N	G	T	G	G	G	T	T/G
02-094964773-M	G	T	G	G	G	T	T/G
02-114758266-N	T	C	T	T	T	C	C/T
02-131136658-M	C	A	C	C	C	A	A/C
02-159897340-M	G	A	G	G	G	A	A/G
02-172504164-G	C	T	C	C	C	T	T/C
03-007561998-N	T	C	T	T	T	C	C/T
03-022347144-G	T	C	T	T	T	C	C/T
03-035115028-M	C	T	C	C	C	T	T/C
03-056067960-G	T	C	T	T	T	C	T/C
03-075336142-M	A	G	A	A	A	G	G/A
03-095186319-G	C	A	C	C	C	A	C/A
03-115468851-N	C	A	C	C	C	A	A/C
03-131286062-N	C	T	C	C	C	T	C/T
03-151125653-M	A	T	A	A	A	T	T/A
04-006370062-M	A	G	A	A	A	G	G/A

04-017015246-M	T	C	T	T	T	C	C/T
04-034965128-M	A	C	A	A	A	C	C/A
04-053894587-M	T	C	T	T	T	C	C/T
04-068252469-M	C	T	C	C	C	T	T/C
04-097015585-M	A	G	A	A	A	G	G/A
04-117567852-N	C	T	C	T/C	C	T	T/C
04-128694339-G	T	G	T	T/G	T	G	T/G
04-142807236-G	G	A	G	A/G	G	A	A/G
05-013136419-M	C	T	T/C	C	C	T	T/C
05-035182717-N	T	G	T	T	T	G	G/T
05-041667588-G	G	T	G	G	G	T	T/G
05-061148036-G	T	C	T	T	T	C	T/C
05-076427870-N	A	G	A	A	A	G	G/A
05-118031699-M	G	A	G	G	G	A	A/G
05-145143884-M	C	T	C	C	C	T	T/C
06-011983883-M	G	C	C/G	C/G	G	C	C/G
06-023207025-M	A	G	G/A	G/A	A	G	G/A
06-038230055-G	A	G	G/A	G/A	A	G	G/A
06-048811360-N	G	T	G	G	G	T	T/G
06-076285738-M	T	A	T	T	T	A	A/T
06-090142535-M	C	A	C	C	C	A	A/C
06-112199886-M	G	T	G	G	G	T	T/G
06-126258422-M	T	C	T	T	T	C	C/T
07-034063244-M	G	A	G	G	G	A	A/G
07-053928010-M	T	G	T	T	T	G	G/T
07-064095712-M	G	T	G	G	G	T	T/G
07-082671949-N	C	G	C	C	C	G	G/C
07-094312514-M	A	G	A	G/A	A	G	G/A
07-112553982-G	T	G	T	T	T	G	T/G
07-124000818-G	T	C	T	T	T	C	T/C
08-015199792-M	T	C	T	T	T	C	C/T
08-032490228-N	A	G	A	A	A	G	G/A
08-053200795-M	T	C	T	T	T	C	C/T
08-065849115-N	A	G	A	A	A	G	G/A
08-088063837-N	C	T	C	C	C	T	T/C
08-101099186-M	A	T	A	A	A	T	T/A
08-117163724-M	G	A	G	G	G	A	A/G
09-017770060-M	T	A	T	T	T	A	A/T

09-029233439-N	A	G	A	A	A	G	A/G
09-037841497-M	T	C	T	T	T	C	C/T
09-063923771-M	G	A	G	G	G	A	A/G
09-084055613-M	C	A	C	C	C	A	A/C
10-008017793-M	A	C	A	A	A	C	C/A
10-028554348-N	G	A	G	G	G	A	G/A
10-053898997-M	G	C	G	G	G	C	C/G
10-060074134-G	G	A	G	G	G	A	A/G
10-077371167-G	G	A	G	G	G	A	A/G
10-099683776-N	C	G	C	C	C	G	G/C
10-120289167-M	A	G	A	A	A	G	G/A
11-004367508-M	G	A	G	G	G	A	A/G
11-022864828-N	C	A	C	C	C	A	A/C
11-033040833-M	T	C	T	T	T	C	C/T
11-061500282-N	T	C	T	T	T	C	C/T
11-077198334-M	G	A	G	G	G	A	A/G
11-098391535-G	T	G	T	T	T	G	G/T
11-113224684-M	A	G	A	A	A	G	G/A
12-009581325-M	G	T	G	G	G	T	T/G
12-031510473-N	G	A	G	G	G	A	A/G
12-049281625-M	C	T	C	C	C	T	T/C
12-064212930-N	A	G	A	A	A	G	A/G
12-106729531-M	T	C	C/T	C/T	T	C	C/T
13-011923617-M	T	C	C/T	C/T	T	C	C/T
13-026482435-G	A	G	G/A	G/A	A	G	G/A
13-037832161-M	A	T	T/A	T/A	A	T	T/A
13-059590161-N	C	T	T/C	T/C	C	T	T/C
13-078326044-G	C	T	C	C	C	T	T/C
13-085133616-G	T	C	T	T	T	C	T/C
13-093046894-N	C	T	C	C	C	T	T/C
13-110566702-N	C	T	C	C	C	T	T/C
13-112696462-N	A	C	A	A	A	C	C/A
14-005055006-M	T	A	T	T	T	A	A/T
14-022368155-G	T	C	T	T	T	C	T/C
14-033881274-G	A	T	A	T/A	A	T	T/A
14-055918382-M	C	T	C	T/C	C	T	T/C
14-079218045-M	C	A	C	A/C	C	A	A/C
14-095233920-G	T	C	T	T	T	C	T/C

14-110887447-M	C	T	C	C	C	T	T/C
15-005994001-M	A	C	A	A	A	C	C/A
15-028279166-G	T	C	T	T	T	C	T/C
15-041919640-N	C	T	C	C	C	T	T/C
15-055206736-N	G	A	G	G	G	A	A/G
15-069647296-G	T	G	T	T	T	G	G/T
15-087100507-M	A	G	A	A	A	G	G/A
15-096231715-M	T	G	T	T	T	G	G/T
16-003310511-N	G	A	G	G	G	A	A/G
16-019621494-C	A	G	A	A	A	G	A/G
16-035239412-C	C	G	C	C	C	G	C/G
16-051080938-C	A	T	T/A	A	A	T	T/A
16-068107787-C	G	A	A/G	G	G	A	A/G
16-093066825-C	T	C		T	T	C	T/C
17-007230139-M	C	G	C	C	C	G	G/C
17-028172639-M	C	T	C	C	C	T	T/C
17-037829090-G	G	T	G	G	G	T	G/T
17-056073815-M	G	A	G	G	G	A	A/G
17-065004394-N	T	C	T	T	T	C	C/T
17-082297869-M	T	G	T	T	T	G	G/T
17-092673068-N	T	G	T	T	T	G	T/G
18-010953833-N	A	G	A	A	A	G	A/G
18-029963387-M	T	C	T	T	T	C	C/T
18-055728214-N	G	C	G	G	G	C	C/G
18-075088655-M	G	A	G	G	G	A	A/G
18-086980249-M	G	A	A/G	G	G	A	A/G
19-003607482-N	C	T	C	C	C	T	T/C
19-013339654-M	A	C	A	A	A	C	C/A
19-034003337-G	G	T	G	G	G	T	T/G
19-046168493-M	G	A	G	G	G	A	A/G
19-060030696-N	A	G	A	A	A	G	G/A
X-016114535-G	C	A	C	C	C	A	A/C
X-022427259-G	C	A	C	C	C	A	C/A
X-034968801-G	G	A	G	G	G	A	A/G
X-042691780-G	T	A	T	T	T	A	T/A
X-054650362-N	T	A	T	T	T	A	A/T
X-074884405-G	A	G	A	A	A	G	A/G
X-087817653-G	A	T	A	A	A	T	T/A

X-109677875-M	A	G	A	A	A	G	G/A
X-123551831-M	A	G	A	A	A	G	G/A
X-143466659-M	A	C	A	A	A	C	C/A

Table 3. Full SNP genome scanning results for MMTV- rtTA mice.

			1	2	B6J	SJL	Het
SNP_ID	Expected SNPs						
Chromosome-bp	C57BL/6J	SJL/J					
01-008110094-M	G	T	G	G	G	T	T/G
01-020235191-G	C	T	C	C	C	T	C/T
01-038984204-M	C	G	G/C	C	C	G	G/C
01-059831398-M	G	T	G	G	G	T	T/G
01-080181487-M	T	A	T	T	T	A	A/T
01-101109196-M	G	C	C/G	C/G	G	C	C/G
01-119177953-M	C	T	T/C	T/C	C	T	T/C
01-139952425-M	A	T	T/A	T/A	A	T	T/A
01-169425148-M	G	T	T/G	T/G	G	T	T/G
01-180301121-G	C	T	T/C	T/C	C	T	T/C
01-191804699-M	A	T	T/A	A	A	T	T/A
02-003179310-M	G	A	G	G	G	A	A/G
02-020551477-M	T	C	T	T	T	C	C/T
02-045952711-G	T	C	T/C	T/C	T	C	T/C
02-064172278-M	C	G	G/C	G/C	C	G	G/C
02-087029735-M	T	C	T	T	T	C	C/T
02-104075364-M	G	C	G	G	G	C	C/G
02-126638575-G	C	T	C	C	C	T	C/T
02-146910375-M	G	A	G	G	G	A	A/G
02-166115846-M	T	C	T	T	T	C	C/T
02-179086475-M	G	T	G	G	G	T	T/G
03-007561998-N	T	C	T	T	T	C	C/T
03-021275532-G	G	A	G	G	G	A	A/G
03-040667523-M	C	T	C	C	C	T	T/C
03-062390782-M	G	A	G	G	G	A	A/G
03-082192100-M	G	A	G	G	G	A	A/G
03-102189723-M	T	G	G/T	G/T	T	G	G/T
03-122263343-G	C	T	T/C	T/C	C	T	T/C
03-138370314-M	C	A	A/C	C	C	A	A/C
03-155372777-M	T	C	C/T	T	T	C	C/T
04-003163167-M	G	T	T/G	G	G	T	T/G
04-022227011-G	C	T	T/C	C	C	T	T/C

04-042020383-M	C	T	T/C	C	C	T	T/C
04-058850394-M	C	T	T/C	C	C	T	T/C
04-086758585-N	A	G	A	A	A	G	G/A
04-102718416-N	C	T	C	C	C	T	T/C
04-122948823-M	A	G	A	A	A	G	G/A
04-142807236-G	G	A	A/G	A/G	G	A	A/G
04-151168886-M	G	T	T/G	T/G	G	T	T/G
05-008305854-N	C	T	T/C	C	C	T	T/C
05-024901514-M	A	G	G/A	G/A	A	G	G/A
05-043353028-N	A	C	A/C	A/C	A	C	A/C
05-062045190-M	C	A	A/C	A/C	C	A	A/C
05-082050497-M	C	A	A/C	C	C	A	A/C
05-103288157-M	T	C	C/T	C/T	T	C	C/T
05-123262990-M	A	G	G/A	G/A	A	G	G/A
05-142017413-M	A	G	G/A	G/A	A	G	G/A
06-003167392-M	C	T	T/C	T/C	C	T	T/C
06-024080365-M	A	G	G/A	G/A	A	G	G/A
06-046967317-M	G	A	A/G	A/G	G	A	A/G
06-060887613-G	A	G	A	G/A	A	G	G/A
06-084596678-G	G	A	A/G	G	G	A	A/G
06-112199886-M	G	T	G	G	G	T	T/G
06-134747045-G	T	C	T	T	T	C	T/C
06-149052281-M	C	G	G/C	C	C	G	G/C
07-011167675-M	C	T	C	C	C	T	T/C
07-032202125-G	A	G	G/A	A	A	G	G/A
07-053928010-M	T	G	G/T	T	T	G	G/T
07-070027360-M	A	C	A	A	A	C	C/A
07-091160556-M	T	C	C/T	T	T	C	C/T
07-112553982-G	T	G	T/G	T/G	T	G	T/G
07-135345950-N	A	G	G/A	G/A	A	G	G/A
08-009110239-M	A	G	A	G/A	A	G	G/A
08-053200795-M	T	C	T		T	C	C/T
08-071925175-M	G	T	G	G	G	T	T/G
08-090088021-M	C	A	A/C	A/C	C	A	A/C
08-109943429-M	C	T	T/C	T/C	C	T	T/C
08-120862827-G	T	C	T	T/C	T	C	T/C
09-010567705-G	T	C	C/T	C/T	T	C	C/T
09-029233439-N	A	G	A	A	A	G	A/G

09-052052234-M	T	C	T	T	T	C	C/T
09-070380686-G	T	C	T	T	T	C	T/C
09-094819555-M	G	A	G	G	G	A	A/G
10-009127141-N	T	C	T	T	T	C	T/C
10-030424407-G	G	A	G/A	G/A	G	A	G/A
10-053898997-M	G	C	C/G	C/G	G	C	C/G
10-070466216-N	A	G	G/A	G/A	A	G	G/A
10-093476458-N	T	C	C/T	C/T	T	C	C/T
10-111395290-G	C	T	T/C	T/C	C	T	T/C
10-129117100-M	G	A	G	G	G	A	A/G
11-011378766-M	G	A	G	G	G	A	A/G
11-030321352-G	C	T	C	C	C	T	C/T
11-051340929-G	T	G	G/T	G/T	T	G	G/T
11-070331570-M	T	C	C/T	C/T	T	C	C/T
11-090199967-M	T	C	T	C/T	T	C	C/T
11-111226923-M	A	C	C/A	C/A	A	C	C/A
12-009581325-M	G	T	T/G	T/G	G	T	T/G
12-029244061-M	G	A	G/A	G/A	G	A	G/A
12-049281625-M	C	T	T/C	T/C	C	T	T/C
12-070670478-M	A	G	G/A	G/A	A	G	G/A
12-092440423-M	G	C	G	G		C	C/G
12-113315003-M	C	G	C	C	C	G	G/C
13-005378755-G	C	T	C	C	C	T	T/C
13-026482435-G	A	G	G/A	G/A	A	G	G/A
13-043995023-N	T	G	G/T	G/T	T	G	G/T
13-065938342-M	G	A	A/G	A/G	G	A	A/G
13-085133616-G	T	C	T/C	T/C	T	C	T/C
13-100574867-N	T	A	T/A	T/A	T	A	T/A
14-006645974-N	T	C	C/T	C/T	T	C	C/T
14-025184538-M	G	A	G/A	G	G	A	G/A
14-046108187-M	G	A	A/G	G	G	A	A/G
14-061541547-N	A	G	G/A	A	A	G	G/A
14-083150973-M	A	G	G/A	A	A	G	G/A
14-103926350-G	T	G	T/G	T/G	T	G	T/G
15-020953071-M	T	C	C/T	T	T	C	C/T
15-046999017-N	A	G	A	A	A	G	G/A
15-069647296-G	T	G	T	T	T	G	G/T
15-088930929-M	G	A	A/G	A/G	G	A	A/G

15-096231715-M	T	G	G/T	G/T	T	G	G/T
16-007016121-C	C	A	C/A	C/A	C	A	C/A
16-031980782-C	A	G	A/G	A/G	A	G	A/G
16-049079612-C	T	C	T	T	T	C	T/C
16-070833511-G	C	T	C/T	C/T	C	T	C/T
16-091028945-C	C	G	C/G	C/G	C	G	C/G
17-010130910-G	T	C	T	C/T	T	C	C/T
17-031242489-M	C	A	C	C	C	A	A/C
17-052179489-M	A	G	A	A	A	G	G/A
17-068191393-M	T	C	T	T	T	C	C/T
17-089136255-M	T	C	T	T	T	C	C/T
18-011819268-M	T	C	C/T	T	T	C	C/T
18-032061772-M	T	G	T	T	T	G	G/T
18-052783850-M	C	T	C	T/C	C	T	T/C
18-072096903-M	T	G	G/T	G/T	T	G	G/T
18-086980249-M	G	A	A/G	A/G	G	A	A/G
19-005218596-N	T	C	T	T	T	C	C/T
19-025120427-M	A	G	A	A	A	G	G/A
19-045460279-N	A	C	A	A	A	C	C/A
19-058179075-M	G	A	A/G	A/G	G	A	A/G
X-016114535-G	C	A	C	C	C	A	A/C
X-035414447-M	T	C	T	T	T	C	C/T
X-046568296-G	A	G	A	A	A	G	A/G
X-063529554-M	C	A	C	C	C	A	A/C
X-088983795-M	T	C	T	T	T	C	C/T
X-109677875-M	A	G	A	A	A	G	G/A